Synthesis, Characterisation and Structure of Mono- and Heteronuclear Nitrido Complexes

***

Synthese, Charakterisierung und Struktur mono- und heteronuklearer Nitridokomplexe

DISSERTATION

der Fakultät für Chemie und Pharmazie
der Eberhard-Karls-Universität Tübingen

zur Erlangung des Grades eines Doktors
der Naturwissenschaften

2005

vorgelegt von

Daniel Morrogh

Tag der mündlichen Prüfung: 2. Dezember 2005

Dekan	Prof. Dr. S. Laufer
1. Berichterstatter	Prof. Dr. Dr. h. c. J. Strähle
2. Berichterstatter	Prof. Dr. E. Schweda

Die vorliegende Arbeit wurde von Februar 2003 bis November 2005 am Institut für Anorganische Chemie der Universität Tübingen angefertigt.

Meinem verehrten Lehrer

Herrn Prof. Dr. Dr. h.c. Joachim Strähle

danke ich sehr herzlich für das Thema dieser Arbeit, seine ständige Gesprächsbereitschaft und die angenehmen Arbeitsbedingungen.

DANKE…

allen Kollegen und Kolleginnen, die zu dem angenehmen und freundschaftlichen Arbeitsklima beitrugen,

besonders danke ich Frau Dr. Cäcilia Maichle-Mössmer, für die wertvollen Diskussionen, Ideen und Geduld,

Herrn Dr. Markus Richter, Frau Dr. Cäcilia Maichle-Mössmer, Herrn Dr. Simon Schwarz und Frau Elke Niquet für die Hilfe bei den Kristallstrukturanalysen,

Frau Rita Raus für die freundliche Hilfe bei der Überwindung bürokratischer Schwierigkeiten,

Herrn Willi Kappler für die Hilfe bei Hard- und Softwareproblemen,

Herrn Dr. Gintaras Pivoriunas für die Hilfe bei der Anfertigung von Corel-Draw-Bildern,

Herrn Dr. J. Glaser, Frau Elke Niquet und Herrn Michael Neukirch für die Hilfe und Unterstützung bei den magnetischen Messungen,

Herrn W. Bock für die Durchführung der Elementaranalysen und Herrn Dr. R. Müller und Herrn H. Bartholomä für die Aufnahme der Massenspektren,

Frau Dr. Cäcilia Maichle-Mössmer und Prof. Dr. Dr.h.c. Joachim Strähle für das Korrekturlesen dieser Arbeit,

Herrn Ingenieur Karl-Heinz Ableitner für seine Hilfsbereitschaft,

Herrn Dr. Markus Richter, Herrn Dr. Simon Schwarz, Herrn Dr. Carlos F. Barboza da Silva und Herrn Dr. Gintaras Pivoriunas für die Ausrichtung des Freitags-Biers,

allen anderen, die hier vergessen wurden.

Für meine Eltern

Index

1. Introduction

The nitrido ligand is, together with the carbine ligand, the strongest known π-electron donor. In the terminal position, the metal-nitrogen bond is characterised as a triple bond [1]. As a result of the π-electron donating, ligands in the *trans*-position to the nitrido fragment are more easily removed or exchanged (*trans*-effect), and the *trans*-ligand metal bonds are longer than comparable *cis*-ligand metal bonds.

Due to their unique properties, nitrido complexes are interesting for a variety of reasons. For medicinal purposes, Technetium complexes with terminal nitrido ligands are used as markers for nuclear medicine [2]. Molybdenum nitrido complexes are used as catalysers for olefin metathesis, and occur naturally in the nitrogen fixing cycling of the certain plants [3].

The aim of this study was to synthesise and characterise new nitrido bridged complexes. This was achieved by the addition of Lewis-acidic complexes of rhodium and iridium to the terminal nitrido ligand of osmium nitrido complexes.

The structural information for the complexes was determined by single-crystal X-ray diffraction, and supported by FT-IR Spectroscopy, Elemental analysis, mass spectroscopy and magnetic measurements.

2. General

The nitrido ligand has many different bonding modes. Figure 2.1 depicts the known bonding modes of the nitrido ligand.

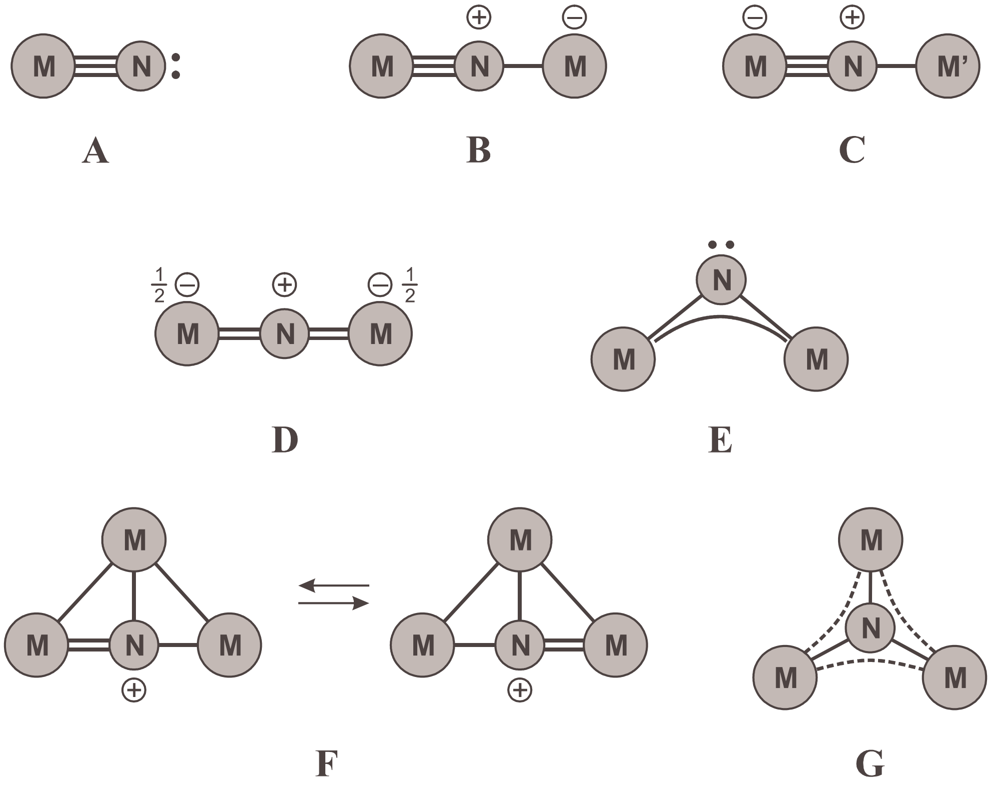

Figure 2.1. The known bonding modes of the nitrido ligand; **A**: terminal; **B**: asymmetric, linear bridge of the donor acceptor type; **C**: asymmetric, linear bridge with a covalent bond; **D**: symmetric, linear bridge; **E**: non-linear bridge; **F**: T-junction bridge; **G**: trigonal planar M_3N unit.

2.1. Terminal Ligand M=N:

In complexes with a terminal nitrido ligand, the (M-N)-bond is extremely short; typically between 166pm (Mo) and 157pm (Ru) [1], and corresponds to a formal triple bond. The (M-N)-bond is made up of one σ- and two mutually perpendicular π-bonds. The two π-bonds result from the overlap of two occupied p-orbitals on the nitrogen with two empty d-orbitals on the metal. The metal is thus usually in a high oxidation state.

2.2. Asymmetric nitrido Bridges

Although the lone pair of electrons on the nitrido ligand exhibit only weakly basic characteristics, under the right conditions it is possible to form a weak bond to other metal centres. This bonding can lead to the formation of polymers (M≡N-M≡N-) such as $ReNCl_4$, and also to tetramers such as $MoNCl_3$ [1]. In both cases the distances between the metal centre and the nitrogen alternates between being short or long. The short (M-N)-bond can be described as a (M≡N)-triple bond, while the longer (M-N)-bond is of the σ-type. In this case the sp-orbital of the nitrogen overlaps with an empty d^2sp^3-orbital of the next metal centre. The hybridised d_{z^2} and p_z orbitals of the metal centre are needed to provide extra σ-electron density for the (M≡N)-triple bond, which results in a weak σ-interaction in the trans-position from the π-bond. Normal σ-interaction takes place in the cis-position from the π-bond. This is the reason why the perpendicular arrangement of long and short (M-N)-distances is preferential. This arrangement leads to the formation of tetrameric molecules, which occur much more frequently than linearly arranged complexes [1].

2.3. Symmetric bridges

Symmetric nitrido briges have to date only occurred in a few two-centre complexes such as $[Nb_2NBr_{10}]^{3-}$ [4] and $K_3[Ru_2NCl_8(OH_2)_2]$ [5]. The (M-N)-bonds can be described as double bonds. In addition to the two σ-bonds, the nitro ligand bonds with the two mutually perpendicular p-orbitals of the nitrogen to form two $d_\pi - p_\pi - d_\pi -$ three centre- π-orbitals, which are filled with a pair of electrons each [1].

2.4. IR-Spectroscopy

IR-Spectroscopy is particularly useful for studying nitrido complexes because the multiple M-N-bonds absorb very strongly in a very characteristic area of the spectrum; for terminal and asymmetrically bridged nitrido complexes this is between 1000 and 1100 cm^{-1}. The absorption bands are also relatively sharp due to the lack of coupling with other vibrations. The longer M-N-bond in asymmetrically bridged complexes is assumed to absorb below 200 cm^{-1} [1].

3. Results and Discussion

3.1. [$(Ph_3As)_2OsNCl_3$]

3.1.1. General

[$OsNCl_4$]$^-$ is the starting material for many osmium complexes. By reacting it with phosphanes it is possible to synthesise many different phosphoraninato-complexes of the form [$Os(NPR_3)Cl_3(PR_3)_2$] where (PR_3= PPh_3, PPh_2Et, $PPhEt_2$ or PPh_2Me) [6]. It is also possible to react [$OsNCl_4$]$^-$ with tertiary arsanes, stibanes and 2,2'-bipyridin to form osmium complexes in the form [L_2OsNCl_3] where (L = Ph_3As, Ph_3Sb or bipy) [6, 7]. The nitrido ligands in these complexes are strongly basic, which is demonstrated by their readiness to form asymmetric nitrido bridges Os≡N-M.

[$(Ph_3As)_2Cl_3OsN$] was first synthesized by W. P. Griffith et al.[6], but no crystal structure was published. [$(Ph_3As)_2Cl_3OsN$] was synthesised and crystals suitable for X-ray analysis were obtained in this work. [$(Ph_3As)_2Cl_3OsN$] was the building block for many of the nitrido complexes described in this thesis. The data from the X-ray analysis proved very useful for investigating and comparing the effects that a nitrido bridge has on the different aspects of a nitrido complex.

3.1.2. Spectroscopic analysis

In the IR-spectrum of $[(Ph_3As)_2Cl_3OsN]$ the Os-N stretch is observed at 1061 cm^{-1}. The Os-Cl vibration occurs at 338 cm^{-1}.

Table 3.1.1. Selected IR vibrations of $[(Ph_3As)_2Cl_3OsN]$.

Vibration	υ(Os≡N)	υ(Os-Cl)
$[(Ph_3As)_2Cl_3OsN]$	1061 st	338 st

In the FAB(+) mass spectrum only the following fragments from the complex $[(Ph_3As)_2Cl_3Os{\equiv}N]$ were identified.

Table 3.1.2. Identifiable peaks from mass spectrum of $[(Ph_3As)_2Cl_3OsN]$.

Peak	Intensity	Fragment
509	5	$[(Ph_3As)OsN]^+$
273	20	$[Cl_2OsN]^+$

3.1.3. Structural Analysis of [$(Ph_3As)_2Cl_3Os{\equiv}N$]

Table 3.1.3. Details from the structural analysis of [$(Ph_3As)_2Cl_3Os{\equiv}N$]

Empirical formula	$C_{36}H_{30}Cl_3NOsAs_2$	
Formula weight [g/mol]	922.7	
Crystal system	triclinic	
Space group	$P\bar{1}$	
Unit cell dimensions [pm] [°]	a = 1183.69(16)	α = 115.497(15)
	b = 1411.03(19)	β = 94.120(16)
	c = 1634.1(2)	γ = 92.033(16)
Volume [pm^3]	$2450 \cdot 10^6$	
Z	3	
Calculated density [g/cm^3]	1.876	
F(000)	1338	
Absorption coefficient [mm^{-1}]	6.186	
Radiation	MoK_α	
Temperature [K]	223	
Crystal size [mm^3]	0.50 x 0.30 x 0.10	
Crystal description	reddish orange blocks	
Diffractometer	STOE, IPDS	
Theta range θ_{max}[°]	28.13	
Index ranges h, k, l	-15 → 15, -18 → 18, -21 → 21	
Reflections collected	30142	
Independent reflections	10999 [R(int) = 0.0636]	
Decay	0	
Refined parameters	582	
Final R indices	R_1 = 0.0402, wR_2 = 0.0856	
GooF	0.874	
Weighting scheme $P = (F_o^2+2F_c^2)/3$	$w = 1/[\sigma^2(F_o^2) + (0.0.445P)^2]$	

Table 3.1.4. Selected bond lengths and bond angles of $[(Ph_3As)_2Cl_3Os{\equiv}N]$

Bond Lengths [pm]			
Os(2)-N(2)	178.1(7)	Os(2)-Cl(22)	246.28(17)
Os(2)-Cl(21)	234.47(14)	Os(2)-As(21)	255.47(8)
Os(2)-Cl(23)	235.21(15)	Os(2)-As(22)	254.16(8)

Bond Angles [º]			
N(2)-Os(2)-Cl(21)	93.34(18)	Cl(21)-Os(2)-As(21)	84.53(5)
N(2)-Os(2)-Cl(23)	96.91(18)	Cl(21)-Os(2)-As(22)	93.41(5)
N(2)-Os(2)-Cl(22)	177.89(18)	Cl(23)-Os(2)-As(21)	96.02(5)
N(2)-Os(2)-As(1)	92.35(17)	Cl(23)-Os(2)-As(22)	85.19(5)
N(2)-Os(2)-As(2)	92.32(17)	Cl(22)-Os(2)-As(21)	87.42(5)
Cl(21)-Os(2)-Cl(23)	169.71(6)	Cl(22)-Os(2)-As(22)	87.85(5)
Cl(21)-Os(2)-Cl(22)	84.55(6)	As(21)-Os(2)-As(22)	175.00(3)
Cl(23)-Os(2)-Cl(22)	85.20(6)		

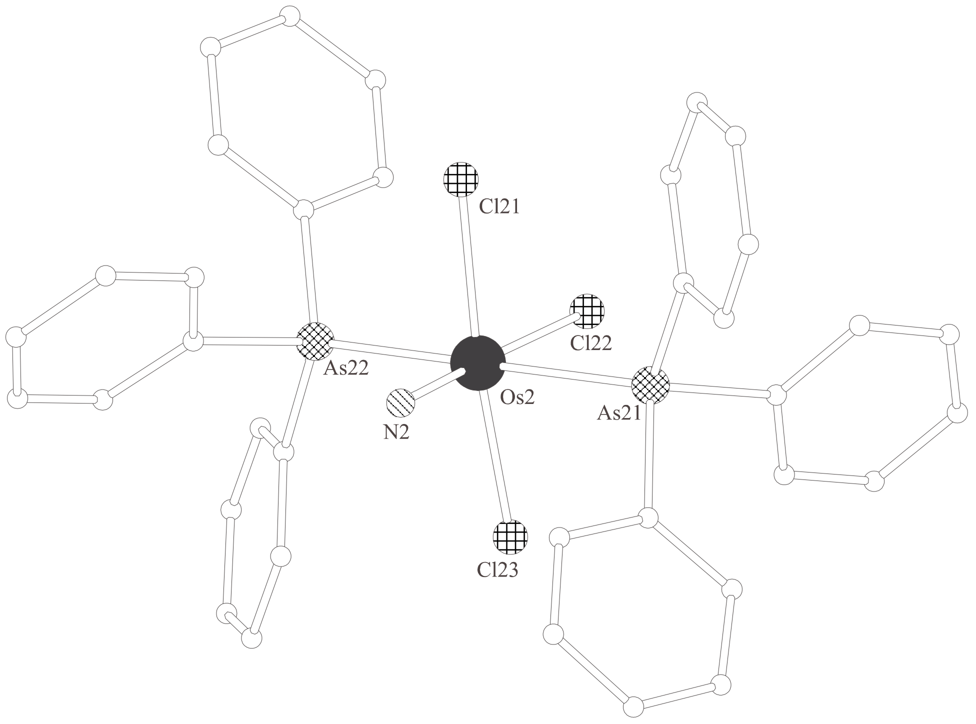

Figure 3.1.1. Crystal structure of $\mathbf{[(Ph_3As)_2Cl_3Os{\equiv}N]}$; the hydrogen atoms have been excluded for clarity.

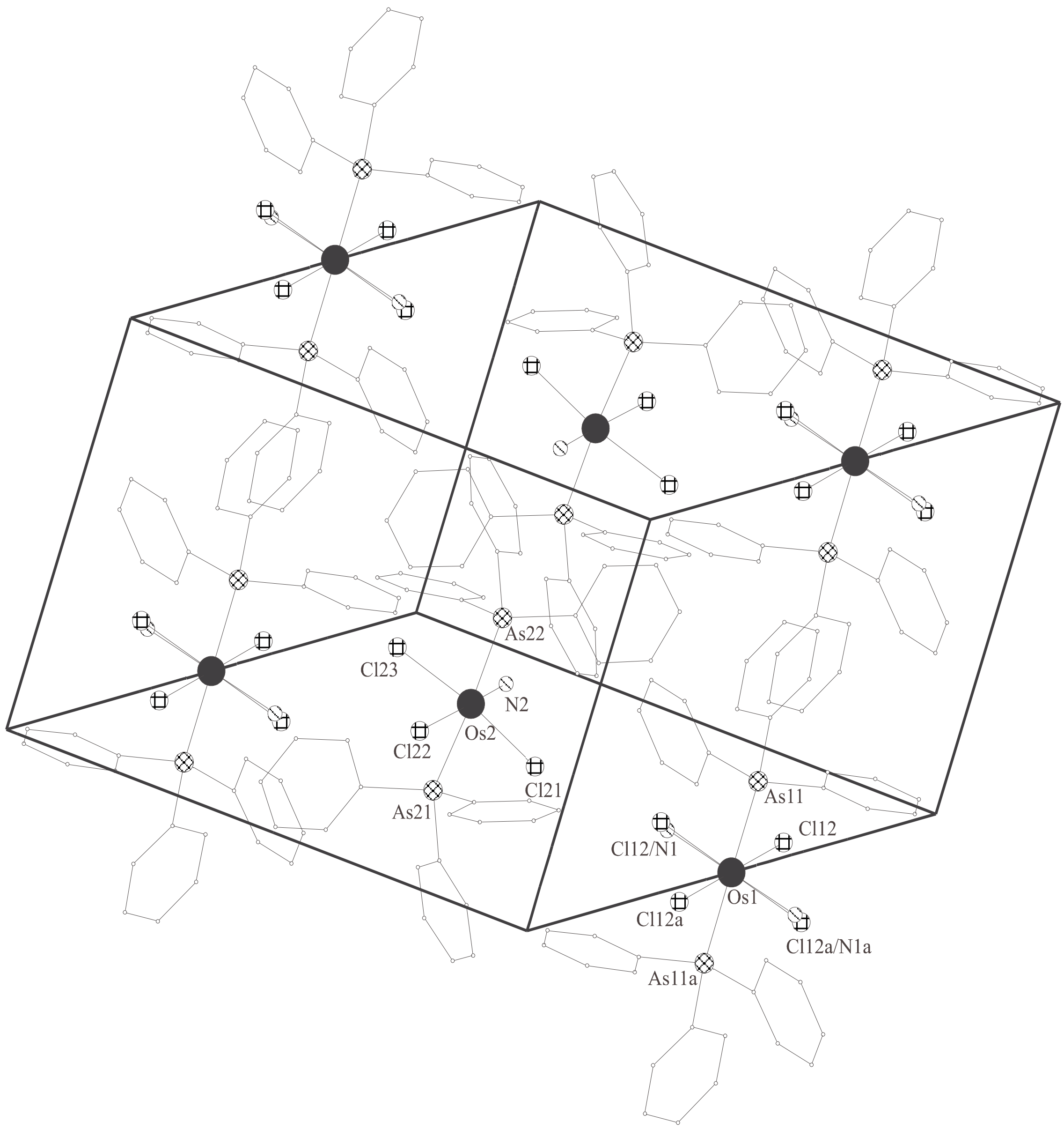

Figure 3.1.2. The P$\bar{1}$ unit cell of **[$(Ph_3As)_2Cl_3Os\equiv N$]**; the symmetry coupled and uncoupled molecules are labelled Os1 and Os2 respectively. In the symmetrically coupled molecules, the split chlorine and nitrido positions are clearly visible and labelled Cl/N.

3.1.4. Discussion and Structure of [$(Ph_3As)_2Cl_3Os{\equiv}N$]

The osmium nitrido complex [$(Ph_3As)_2Cl_3Os{\equiv}N$] crystallises in the triclinic space group $P\bar{1}$ with three [$(Ph_3As)_2Cl_3Os{\equiv}N$] molecules per unit cell. The octahedrally-coordinated osmium atom has three chlorine ligands, one in *trans*-position to the nitrido ligand, and the other two mutually *trans*- to each other in the same plane as the two mutually *trans*- triphenyl arsane ligands.

The X-ray structure was solved in the space group $P\bar{1}$, with three [$(Ph_3As)_2Cl_3Os{\equiv}N$] molecules per unit cell. It follows that one of the molecules occupies a symmetry centre (See figure 3.1.2.). The osmium atom was found on an inversion centre C_i, and this element of symmetry posed a problem for the solution of the X-ray structure, because the compound does not have an inversion centre. The problem was resolved by splitting the positions of the chlorine and nitrogen atoms; meaning that they both simultaneously occupy both sides. The Os(2)-N(2)-bond length of 178.1(7) pm in this solution of the crystal structure is much too long for a terminal nitrido compound of this class; a similar nitrido compound, $ReNCl_2(PMe_2Ph)_3$, has a Re-N-bond length of 166.0 pm [8]. This is reinforced by the fact that the Os-N-bond lengths in the nitrido bridged compounds [$(Ph_3As)_2Cl_3Os{\equiv}N$-RhCl(COD)] and [$(Ph_3As)_2Cl_3Os{\equiv}N$-IrCl(COD)], at 167.6 pm and 171.2 pm respectively, are considerably shorter than the un-bridged terminal Os-N-bond length, which is not possible.

It was assumed that this problem could be resolved by solving the structure in the space group P1, where the lack of symmetry should facilitate the separation of the two atomic positions. This solution gave an Os-N-bond length of 168 pm, which is more realistic for a terminal nitrido complex. Unfortunately it was not possible to anisotropically refine the crystal structure in the space group P1, and the R-values and the anisotropic temperature factors were unacceptably high.

This problem led to the presumption that the nitrogen position alternates with the chlorine in the crystal, therefore making X-ray structural analysis difficult.

3.1.5. Magnetic Properties of [$(Ph_3As)_2Cl_3Os{\equiv}N$]

As expected, due to the formal +VI oxidation state of the octahedrally coordinated Osmium in [$(Ph_3As)_2Cl_3Os{\equiv}N$], the nitrido complex is diamagnetic, with a molar susceptibility of $-1.01\cdot10^{-3}$ emu/mol at 295 K.

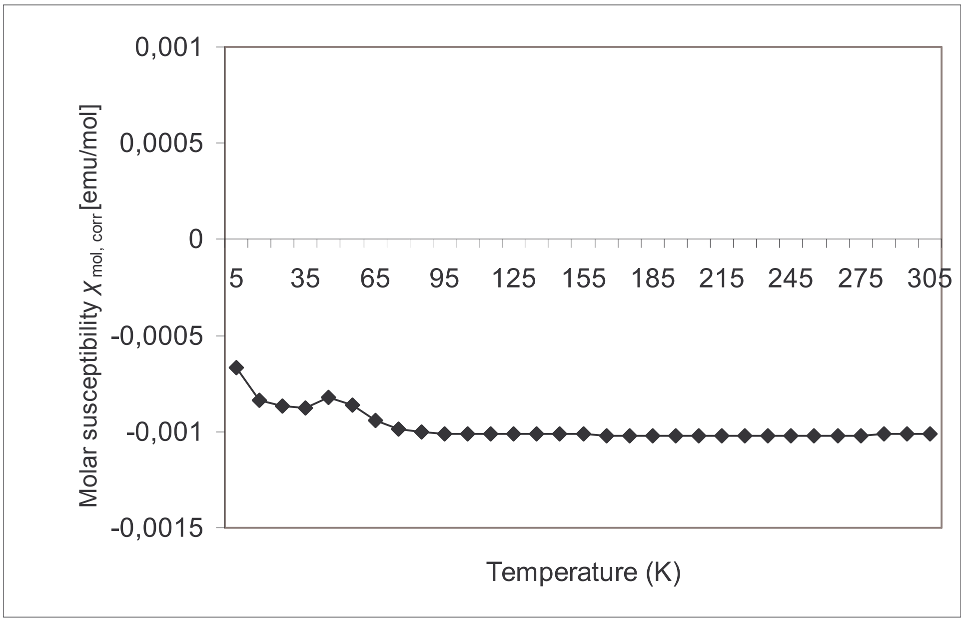

Figure 3.1.3. Magnetic susceptibility $\chi_{\mathrm{mol,\,corr}}$ of **[$(Ph_3As)_2Cl_3Os{\equiv}N$]** as a function of temperature.

3.2. [$(Ph_3As)_2Cl_3Os{\equiv}N\text{-}RhCl(COD)$]

3.2.1. General

The strongly basic nitrido ligand of [$(Ph_3As)_2OsNCl_3$] is ideally suited to react with suitable Lewis acids. In this case the nitrido complex reacts with the dimeric compound, [$Rh(\mu\text{-}Cl)(COD)]_2$, breaking the chloro bridge to form an asymmetric nitrido bridge to the rhodium atom. The lone pair of electrons on the nitrogen coordinates to the position left free by the departing chlorine atom of the chloro bridge. This is a very practical method for synthesising nitrido bridges.

3.2.2. Spectroscopic Analysis

In the IR-spectrum of [$(Ph_3As)_2Cl_3Os{\equiv}N\text{-}RhCl(COD)$] the Os≡N absorption is observed at 1048 cm^{-1}. The Os-Cl stretch occurs at 335.2 cm^{-1}.

Table 3.2.1. Selected IR vibrations of [$(Ph_3As)_2Cl_3Os{\equiv}N\text{-}RhCl(COD)$].

Vibration	υ(Os≡N)	υ(Os-Cl)
[$(Ph_3As)_2Cl_3OsN$]	1075 st	338 st
[$(Ph_3As)_2Cl_3Os{\equiv}N\text{-}RhCl(COD)$]	1048 st	335 st

In the FAB(+) mass spectrum only two fragments from the complex [(Ph$_3$As)$_2$Cl$_3$Os≡N-RhCl(COD)] were identified. Due to the fragility for the nitrido bridge, no bridged complex fragments were found,

Table 3.2.2. Identifiable peaks from the FAB(+) mass spectrum of [(Ph$_3$As $_2$Cl$_3$Os≡N-RhCl(COD)]

Peak	Intensity	Fragment
887	5	[(Ph$_3$As)$_2$Cl$_2$OsN]$^+$
579	5	[(Ph$_3$As)Cl$_2$OsN]$^+$

3.2.3. Structural Analysis of [$(Ph_3As)_2Cl_3Os{\equiv}N\text{-}RhCl(COD)$]

Table 3.2.3. Details from the structural analysis of [$(Ph_3As)_2Cl_3Os{\equiv}N\text{-}RhCl(COD)$]

Empirical formula	$C_{44}H_{42}Cl_4NOsRhAs_2$	
Formula weight [g/mol]	1169.54	
Crystal system	monoclinic	
Space group	Cc	
Unit cell dimensions [pm] [º]	a = 2316.8(5)	$\alpha = 90$
	b = 1169.31(11)	$\beta = 106.121(11)$
	c = 1601.35(17)	$\gamma = 90$
Volume [pm^3]	$4167.6(10)\cdot10^6$	
Z	4	
Calculated density [g/cm^3]	1.864	
F(000)	2272	
Absorption coefficient [mm^{-1}]	13.245	
Radiation	CuK_α	
Temperature [K]	223	
Crystal size [mm^3]	0.25 x 0.25 x 0.05	
Crystal description	Olive brown blocks	
Diffractometer	CAD4, Enraf-Nonius	
Measurement method	ω-Scans	
Theta range θ_{max}[º]	65.07	
Index ranges h, k, l	-27 → 27, -1 → 13, -18 → 18	
Reflections collected	7550	
Independent reflections	6782 [R(int) = 0.0617]	
Decay	0	
Refined parameters	479	
Final R indices	$R_1 = 0.0558$, $wR_2 = 0.1452$	
GooF	1.098	
Weighting scheme $P = (F_o^2+2F_c^2)/3$	$w = 1/[\sigma^2(F_o^2)+(0.0854P)^2+58.1185P]$	
Absorption correction	DIFABS	
T_{min}, T_{max}	0.047; 0.465	

Table 3.2.4. Selected bond lengths and bond angles of $[(Ph_3As)_2Cl_3Os\equiv N\text{-}RhCl(COD)]$

Bond Lengths [pm]			
Os-N	167.6(10)	Rh-Cl(4)	235.0(4)
Rh-N	185.5(10)	Os-Cl(1)	237.3(5)
Rh-C(1)	227.6(18)	Os-Cl(2)	238.0(5)
Rh-C(2)	230(2)	Os-Cl(3)	241.5(3)
Rh-C(5)	210.4(17)	Os-As(1)	253.1(2)
Rh-C(6)	213.4(17)	Os-As(2)	254.6(2)
C(1)-C(2)	139(3)	C(5)-C(6)	141(2)
C(2)-C(3)	148(3)	C(6)-C(7)	150(2)
C(3)-C(4)	150(3)	C(7)-C(8)	157(3)
C(4)-C(5)	153(2)	C(1)-C(8)	148(3)

Bond Angles [º]			
Os-N-Rh	176.1(7)	N-Rh-Cl (4)	88.9(4)
N-Os-Cl(1)	95.0(4)	N-Rh-C(1)	167.5(7)
N-Os-Cl(2)	92.0(4)	N-Rh-C(2)	157.2(7)
N-Os-Cl(3)	177.7(5)	N-Rh-C(5)	91.1(5)
N-Os-As(1)	96.7(5)	N-Rh-C(6)	98.2(6)
N-Os-As(2)	92.5(5)	C(1)-Rh-Cl(4)	88.3(6)
Cl(1)-Os-Cl(2)	172.90(15)	C(2)-Rh-Cl(4)	92.9(5)
Cl(1)-Os-Cl(3)	87.2(2)	C(5)-Rh-Cl(4)	162.0(5)
Cl(1)-Os-As(1)	84.99(14)	C(6)-Rh-Cl(4)	158.6(5)
Cl(1)-Os-As(2)	93.58(14)	C(1)-Rh-C(2)	35.3(7)
Cl(2)-Os-Cl(3)	85.69(19)	C(1)-Rh-C(5)	95.3(7)
Cl(2)-Os-As(1)	94.60(16)	C(1)-Rh-C(6)	80.4(8)
Cl(2)-Os-As(2)	85.70(16)	C(2)-Rh-C(5)	80.3(7)
Cl(3)-Os-As(1)	84.05(19)	C(2)-Rh-C(6)	88.3(6)
Cl(3)-Os-As(2)	86.81(19)	C(5)-Rh-C(6)	38.8(7)
As(1)-Os-As(2)	170.80(5)		

Bond Angles [º]			
C(1)-C(2)-C(3)	123(2)	C(5)-C(6)-C(7)	123.2(15)
C(2)-C(3)-C(4)	116.5(17)	C(6)-C(7)-C(8)	112.9 (15)
C(3)-C(4)-C(5)	113.0(15)	C(7)-C(8)-C(1)	113.5(17)
C(4)-C(5)-C(6)	124.3(15)	C(8)-C(1)-C(2)	127(2)

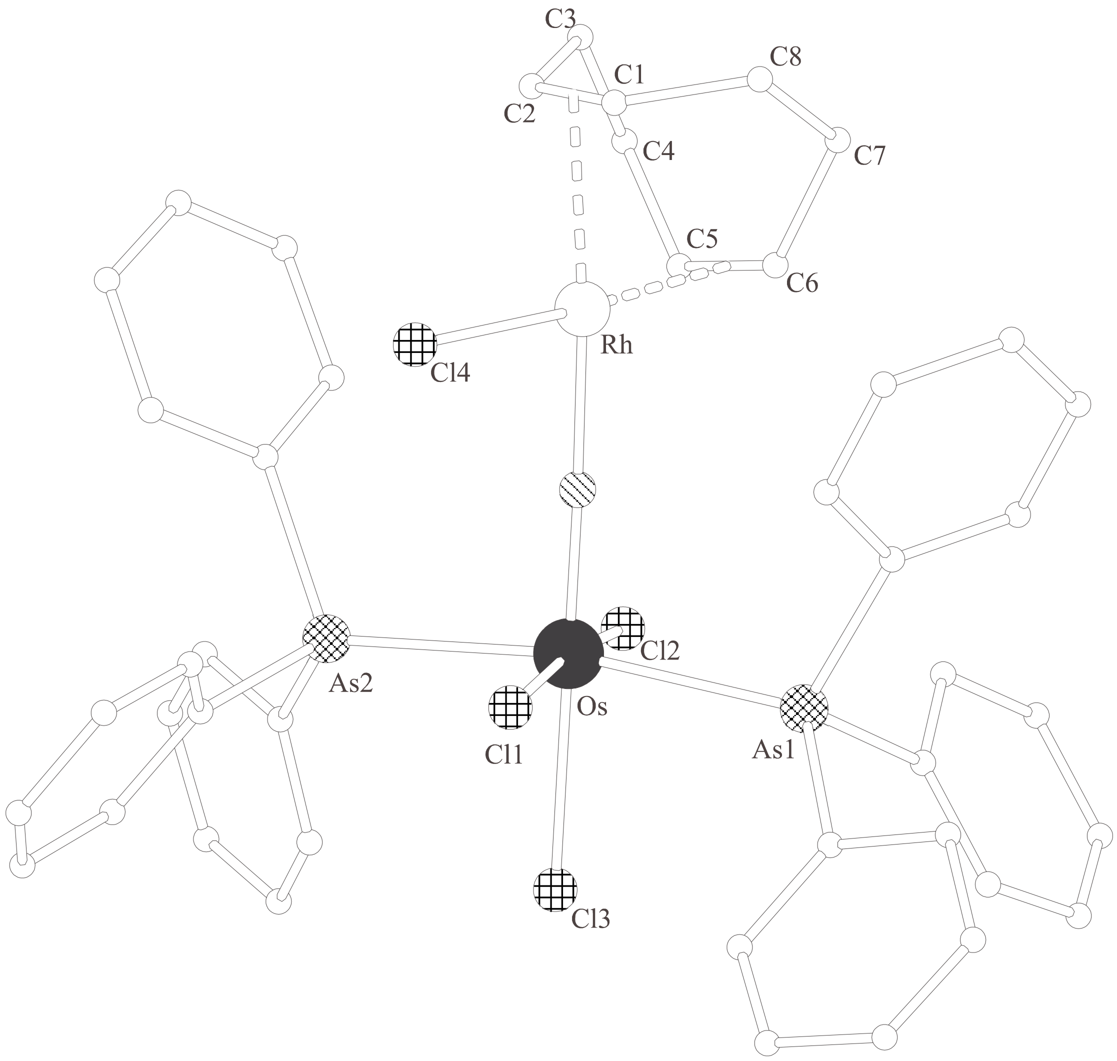

Figure 3.2.1. Crystal structure of **[(Ph$_3$As)$_2$Cl$_3$Os≡N-RhCl(COD)]**; the hydrogen atoms have been excluded for clarity.

3.2.4. Discussion and Structure of [$(Ph_3As)_2Cl_3Os{\equiv}N$-RhCl(COD)]

The dinuclear complex, [$(Ph_3As)_2Cl_3Os{\equiv}N$-RhCl(COD)], crystallizes in the monoclinic space group Cc, with 4 molecules in the unit cell. The nitrido complex [$(Ph_3As)_2Cl_3Os{\equiv}N$] coordinates to the RhCl(COD) fragment by forming a nitrido bridge. The monovalent rhodium atom attains quadratic planar geometry, with the π-bonds of the cycloocatdiene ligand mutually *cis*- to one another. The octahedrally-coordinated osmium atom has three chloro ligands, one in *trans*-position to the nitrido ligand, and the other two mutually *trans*- to each other in the same plane as the two mutually *trans*- (Ph_3As) ligands. This geometry was to be expected because the chlorine and (Ph_3As) ligands are similarly arranged in the starting material, [$(Ph_3As)_2Cl_3Os{\equiv}N$].

The nitrido brige is almost linear with an Os-N-Rh angle of 176.1(7)°. The Os-N-bond length at 167.6(10) pm corresponds to an Os-N triple bond. A similar Os-N-bond length was found in [$(Ph_3Sb)_2Cl_3Os{\equiv}N$-RhCl(COD)] [9], the stibane analogue to this compound, with a Os-N-bond length of 168.3(7) pm. The Rh-N-bond length at 185.5(10) pm is much shorter than the sum of the covalent radii of the two atoms as given by Pauling [10]. The Rh-C-bond lengths to the cyclooctadiene fragment are markedly longer in *trans*-position to the nitrido bridge, 227.6(18) and 230(2) pm, when compared to those in *cis*-position, 213.4(17) and 210.4(17) pm, indicating a π-component to the Rh-N-bond. The nitrido bridge also affects the Os-Cl-bond length in *trans*-position to the nitrido ligand, where the Os-Cl-bond is about 3 pm longer than those in *cis*-position. This difference is notably less than *trans*- *cis*- Os-Cl-bond length difference in the starting material, [$(Ph_3As)_2Cl_3Os{\equiv}N$], where the Os-Cl-bond length in *trans*-position is 11 pm longer than those in *cis*-position. This indicates that in the dinuclear complex there is a slight reduction in the Os-N-bond order, which is reflected in the differing Os-Cl-bond lengths in the nitrido bridged, and un-bridged complexes.

3.2.5. Magnetic Properties of [(Ph$_3$As)$_2$Cl$_3$Os≡N-RhCl(COD)]

The octahedral environment of the osmium atom entails that it has a +VI formal oxidation state, this, coupled with the quadratic planar geometry of the rhodium atom means that the complex was expected to be diamagnetic. This was confirmed by the SQUID magnetic measurement, with a molar susceptibility of $-1.47 \cdot 10^{-3}$ emu/mol at 295 K.

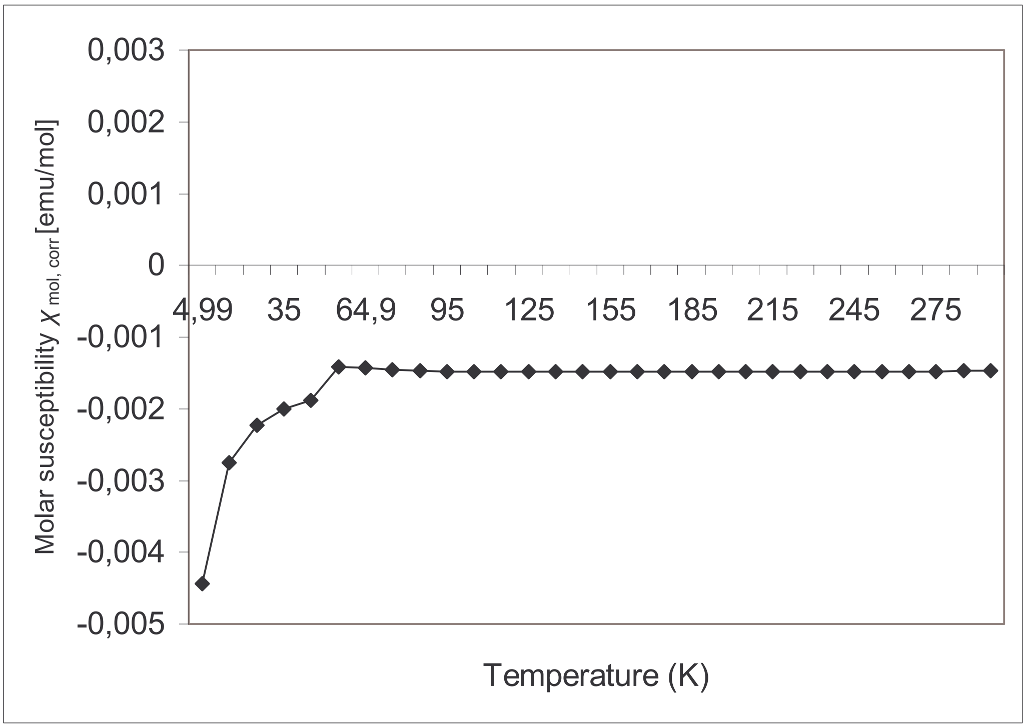

Figure 3.2.2. Magnetic susceptibility $\chi_{mol, corr}$ of **[(Ph$_3$As)$_2$Cl$_3$Os≡N-RhCl(COD)]** as a function of temperature.

3.3. [$(Ph_3As)_2Cl_3Os{\equiv}N$-IrCl(COD)]

3.3.1. General

The nitrido ligand of [$(Ph_3As)_2OsNCl_3$] reacts with the dimeric iridium compound [Ir(μ-Cl)(COD)]$_2$ in a similar fashion to the rhodium analogue, described in the previous section, with the strongly basic nitrido ligand of [$(Ph_3As)_2OsNCl_3$] breaking the chloro bridge of the iridium dimer to form an asymmetrically bridged nitrido complex [$(Ph_3As)_2Cl_3Os{\equiv}N$-IrCl(COD)]. The complex is isostructural to the rhodium analogue, and crystallises in the same monoclinic space group Cc.

3.3.2. Spectroscopic Analysis

In the IR-spectrum of [$(Ph_3As)_2Cl_3Os{\equiv}N$-IrCl(COD)] the Os≡N absorption is observed at 1063 cm^{-1}. The Os-Cl stretch occurs at 334.2 cm^{-1}. The absorption of the bridged Os≡N bond is lower than that of the unbridged Os≡N bond, which corresponds to a reduction in the Os-N-bond order, and an increase in the Os-N-bond length.

Table 3.3.1. Selected IR vibrations of [$(Ph_3As)_2Cl_3Os{\equiv}N$-IrCl(COD)]

Vibration	υ(Os≡N)	υ(Os-Cl)
[$(Ph_3As)_2Cl_3OsN$]	1075 st	338 st
[$(Ph_3As)_2Cl_3Os{\equiv}N$-RhCl(COD)]	1063 w	334 w

In the FAB(+) mass spectrum only the following fragments from the complex $[(Ph_3As)_2Cl_3Os{\equiv}N\text{-}IrCl(COD)]$ were identified. No bridged complex fragments were found due to the fragility of the nitrido bridge.

Table 3.3.2. Identifiable peaks from the FAB(+) mass spectrum of $[(Ph_3As)_2Cl_3Os{\equiv}N\text{-}IrCl(COD)]$

Peak	Intensity	Fragment
579	5	$[(Ph_3As)Cl_2OsN]^+$
338	10	$[ClIr(COD)]^+$
273	20	$[Cl_2OsN]^+$
229	25	$[IrCl]^+$

3.3.3. Structural Analysis of [$(Ph_3As)_2Cl_3Os\equiv N$-IrCl(COD)]

Table 3.3.3. Details from the structural analysis of [$(Ph_3As)_2Cl_3Os\equiv N$-IrCl(COD)]

Empirical formula	$C_{44}H_{42}Cl_4NOsIrAs_2$	
Formula weight [g/mol]	1258.83	
Crystal system	Monoclinic	
Space group	Cc	
Unit cell dimensions [pm] [º]	a = 2322.1(2)	$\alpha = 90$
	b = 1167.01(6)	$\beta = 105.927(9)$
	c = 1603.77(18)	$\gamma = 90$
Volume [pm^3]	$4179.3\cdot10^6$	
Z	4	
Calculated density [g/cm^3]	2.001	
F(000)	2400	
Absorption coefficient [mm^{-1}]	16.089	
Radiation	CuK_α	
Temperature [K]	223	
Crystal size [mm^3]	0.30 x 0.20 x 0.15	
Crystal description	Olive/brown blocks	
Diffractometer	CAD4, Enraf-Nonius	
Measurement method	ω-Scans	
Theta range θ_{max}[º]	65.07	
Index ranges h, k, l	-27 → 27, -1 → 13, -18 → 18	
Reflections collected	7451	
Independent reflections	7100 [R(int) = 0.0334]	
Decay	0	
Refined parameters	479	
Final R indices	$R_1 = 0.0433$, $wR_2 = 0.0994$	
GooF	0.997	
Weighting scheme $P = (F_o^2+2F_c^2)/3$	$w = 1/[\sigma^2(F_o^2)+(0.464P)^2+81.2853P]$	
Absorption correction	DIFABS	
T_{min}, T_{max}	0.187; 0.658	

Table 3.3.4. Selected bond lengths and bond angles of [$(Ph_3As)_2Cl_3Os\equiv N\text{-}IrCl(COD)$]

Bond Lengths [pm]			
Os-N	171.2(8)	Ir-Cl(4)	239.0(3)
Ir-N	181.5(8)	Os-Cl(1)	238.0(4)
Ir-C (1)	229.7 (18)	Os-Cl(2)	237.6(4)
Ir-C(2)	226(3)	Os-Cl(3)	241.5(3)
Ir-C(5)	206.7(16)	Os-As(1)	252.8(2)
Ir-C(6)	202.6(14)	Os-As(2)	254.3(2)
C(1)-C(2)	102(6)	C(5)-C(6)	145(2)
C(2)-C(3)	174(6)	C(6)-C(7)	148(2)
C(3)-C(4)	151(3)	C(7)-C(8)	151(3)
C(4)-C(5)	154(2)	C(1)-C(8)	129(4)

Bond Angles [º]			
Os-N-Ir	176.2(8)	N-Ir-Cl(4)	90.1(4)
N-Os-Cl(1)	93.7(4)	N-Ir-C(1)	158.6(7)
N-Os-Cl(2)	92.7(4)	N-Ir-C(2)	175.0(16)
N-Os-Cl(3)	178.8(6)	N-Ir-C(5)	98.2(6)
N-Os-As(1)	95.6(6)	N-Ir-C(6)	92.2(6)
N-Os-As(2)	93.2(6)	Cl(4)-Ir-C(1)	97.5(11)
Cl(1)-Os-Cl(2)	173.59(11)	Cl(4)-Ir-C(2)	86.2(6)
Cl(1)-Os-Cl(3)	86.6(2)	Cl(4)-Ir-C(5)	157.7(4)
Cl(1)-Os-As(1)	85.55(13)	Cl(4)-Ir-C(6)	159.3(4)
Cl(1)-Os-As(2)	93.65(13)	C(1)-Ir-C(2)	25.9(16)
Cl(2)-Os-Cl(3)	86.97(19)	C(1)-Ir-C(5)	82.3(11)
Cl(2)-Os-As(1)	94.28(12)	C(1)-Ir-C(6)	73.8(11)
Cl(2)-Os-As(2)	85.54(12)	C(2)-Ir-C(5)	84.2(8)
Cl(3)-Os-As(1)	85.5(2)	C(2)-Ir-C(6)	92.4(11)
Cl(3)-Os-As(2)	85.7(2)	C(5)-Ir-C(6)	41.5(6)
As(1)-Os-As(2)	171.23(4)		

Bond Angles [º]			
C(1)-C(2)-C(3)	117(3)	C(5)-C(6)-C(7)	123.5(14)
C(2)-C(3)-C(4)	111(2)	C(6)-C(7)-C(8)	113.8(14)
C(3)-C(4)-C(5)	110.6(14)	C(7)-C(8)-C(1)	111.2(16)
C(4)-C(5)-C(6)	120.9(13)	C(8)-C(1)-C(2)	147(4)

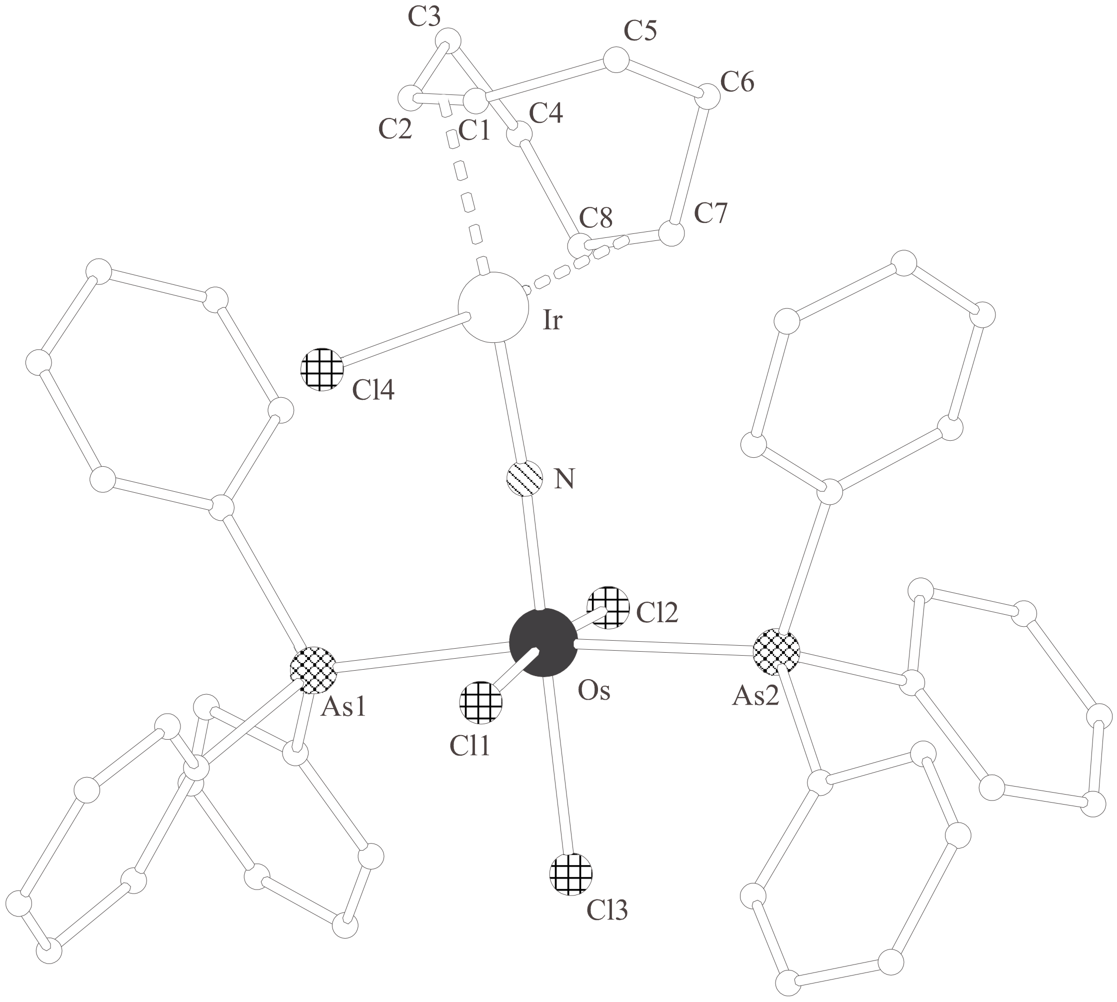

Figure 3.3 Crystal structure of **$[(Ph_3As)_2Cl_3Os\equiv N\text{-}IrCl(COD)]$**; the hydrogen atoms have been excluded for clarity.

3.3.4. Discussion and Structure of [(Ph$_3$As)$_2$Cl$_3$Os≡N-IrCl(COD)]

The dinuclear complex, [(Ph$_3$As)$_2$Cl$_3$Os≡N-IrCl(COD)], crystallises in the monoclinic space group Cc, with 4 [(Ph$_3$As)$_2$Cl$_3$Os≡N-IrCl(COD)] molecules in the unit cell. In this asymmetrically nitrido-bridged complex, the starting material, [(Ph$_3$As)$_2$Cl$_3$Os≡N], coordinates to the IrCl(COD) fragment by forming a nitrido bridge. The monovalent iridium atom attains quadratic planar geometry, with both π-bonds of the cycloocatdiene ligand in *cis*-position. The osmium atom is octahedrally coordinated, with three chloro ligands; one in *trans*-position to the nitrido bridge, and the other two mutually *trans*- to one another, and occupying the same plane as the two mutually *trans*- (Ph$_3$As) ligands. This geometry was to be expected, firstly due to the geometry of the starting material, [(Ph$_3$As)$_2$Cl$_3$Os≡N], and secondly because of the similarities between this complex and the rhodium analogue described in the previous chapter.

The nitrido bridge exhibits near linearity with an Os-N-Ir angle of 176.2(8)°. The Os-N-bond length at 171.2(8) pm corresponds to an Os-N triple bond. A similar Os-N-bond length was found in [(Ph$_3$Sb)$_2$Cl$_3$Os≡N-IrCl(COD)], the stibane analogue to this compound, with a Os-N-bond length of 171(2) pm (Chapter **3.5**). The Ir-N-bond length at 181.5(8) pm is much shorter than the sum of the covalent radii of the two atoms as given by Pauling [10]. The Ir-C-bond lengths to the cyclooctadiene fragment are, as in the other complexes, also influenced by their position with regard to the nitrido bridge. The bonds in *trans*-position to the nitrido bridge being markedly longer, 226(3) and 229.7(18) pm, than those in cis-position; 202.6(14) and 206.7(16) pm, this difference in bond lengths suggests a π-component to the Ir-N-bond. The influence of the nitrido bridge is also noted in the differing Os-Cl-bond lengths about the osmium centre, where the Os-Cl-bond length in *trans*-position, is 3.5 pm longer than those in *cis*-position with respect to the nitrido bridge.

3.3.5. Magnetic Properties of [$(Ph_3As)_2Cl_3Os{\equiv}N$-IrCl(COD)]

The octahedral environment of the osmium centre entails that it has a +VI formal oxidation state, this, coupled with the quadratic planar geometry of the iridium centre means that the complex was expected to be diamagnetic. This was confirmed by a SQUID magnetic measurement, with a molar susceptibility of $-9.14 \cdot 10^{-4}$ emu/mol at 295 K.

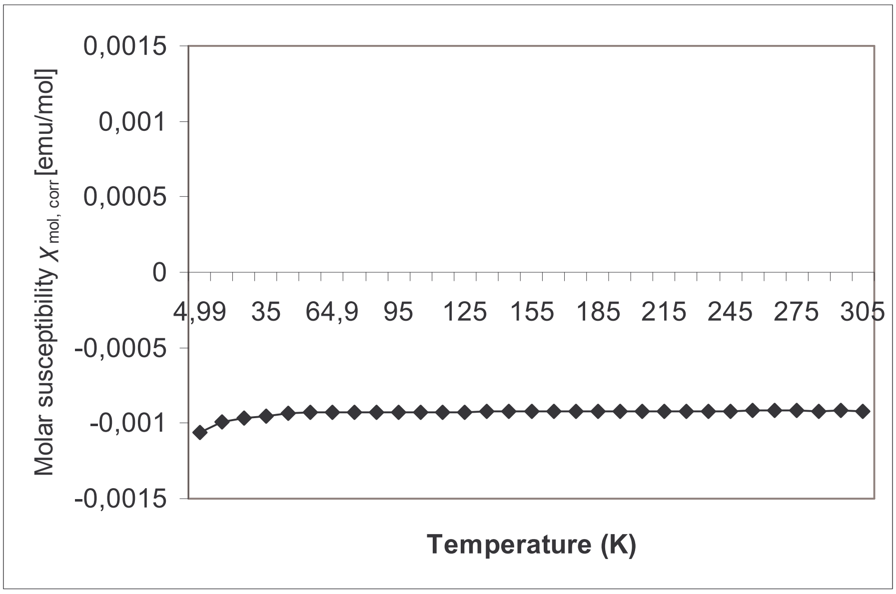

Figure 3.3.2. Magnetic susceptibility $\chi_{\mathrm{mol,\ corr}}$ of **[$(Ph_3As)_2Cl_3Os{\equiv}N$-IrCl(COD)]** as a function of temperature.

3.4. $[(H_2O)Cl_4Os{\equiv}N\text{-}IrClCp^*(Ph_3As)]{\cdot}(H_2O)$

3.4.1. General

The nitrido ligand of $[(Ph_3As)_2OsNCl_3]$ reacts in the presence of water with the dimeric iridium compound $[IrCl_2(Cp^*)]_2$, with the nitrido ligand of $[(Ph_3As)_2OsNCl_3]$ breaking the chloro bridge of the iridium complex to form an asymmetrically bridged nitrido complex $[(H_2O)Cl_4Os{\equiv}N\text{-}IrClCp^*(Ph_3As)]{\cdot}(H_2O)$. Interestingly, one of the triphenyl-arsane ligands on the osmium atom migrates to the iridium, where it takes the place of a chloro ligand. The displaced chlorine atom migrates to the free position left by the triphenyl-arsane ligand on the osmium atom. The second triphenyl-arsane ligand also leaves the osmium atom, presumably taking part in a tandem reaction (shown below) with an $IrCl_2(Cp^*)$ fragment.

$$\left[(Ph_3As)_2OsNCl_3\right] + \left[IrCl_2(Cp^*)\right]_2 \xrightarrow{H_2O}$$

$$\left[(H_2O)Cl_4Os \equiv N - IrClCp^*(Ph_3As)\right]\cdot(H_2O) + IrCl_2Cp^*(Ph_3As)$$

A similar reaction occurs in the synthesis of the Rh- analogue of this complex, described in **3.7.**, the difference being that the nitrido bridged complex was not isolated, only the rhodium by-product.

3.4.2. Spectroscopic Analysis

In the IR-spectrum of [$(H_2O)Cl_4Os\equiv N$-IrClCp*(Ph_3As)]•(H_2O) the Os≡N absorption is observed at 1074.96 cm^{-1}. The Os-Cl stretch occurs at 333.93 cm^{-1}. The Os≡N stretch is lower then the Os≡N absorption of the unbridged [PPh_4][$OsNCl_4$] at 1123 cm^{-1} [11]. This corresponds to a decrease in the Os-N-bond order, and an increase in the Os-N-bond length from 150 pm in the unbridged complex to 168 pm in bridged complex.

Table 3.4.1. Selected IR vibrations of [$(H_2O)Cl_4Os\equiv N$-IrClCp*(Ph_3As)]·(H_2O)

Vibration	υ(Os≡N)	υ(Os-Cl)
[PPh_4][$OsNCl_4$] [11]	1123 st	338 st
[$(H_2O)Cl_4Os\equiv N$-IrClCp*(Ph_3As)].(H_2O)	1075 st	334 st

In the FAB(+) mass spectrum only the following fragments from the complex [$(H_2O)Cl_4Os\equiv N$-IrClCp*(Ph_3As)]•(H_2O) were identified. No bridged complex fragments were found.

Table 3.4.2. Identifiable peaks from the FAB(+) mass spectrum of [$(H_2O)Cl_4Os\equiv N$-IrClCp*(Ph_3As)]•(H_2O)

Peak	Intensity	Fragment
666	5	[(Ph_3As)IrClCp*]$^+$
327	10	[IrClCp*]$^+$
273	20	[Cl_2OsN]$^+$

3.4.3. Structural Analysis of $[(H_2O)Cl_4Os{\equiv}N\text{-}IrClCp^*(Ph_3As)]\cdot(H_2O)$

Table 3.4.3. Details from the structural analysis of $[(H_2O)Cl_4Os{\equiv}N\text{-}IrClCp^*(Ph_3As)]\cdot(H_2O)$

Empirical formula	$C_{28}H_{34}Cl_5NOsIrAsO_2$	
Formula weight [g/mol]	1051.13	
Crystal system	monoclinic	
Space group	Cm	
Unit cell dimensions [pm] [º]	a = 1105.53(6)	α = 90
	b = 1486.76(9)	β = 97.191(4)
	c = 2024.88(10)	γ = 90
Volume [pm^3]	$3302.0(3)\cdot10^6$	
Z	4	
Calculated density [g/cm^3]	2.114	
F(000)	1984	
Absorption coefficient [mm^{-1}]	9.296	
Radiation	MoK_α	
Temperature [K]	173	
Crystal size [mm^3]	0.25 x 0.20 x 0.05	
Crystal description	Green platelets	
Diffractometer	STOE, IPDS	
Theta range θ_{max}[º]	24.71	
Index ranges h, k, l	-13 → 13, -17 → 17, -21 → 23	
Reflections collected	19294	
Independent reflections	5599 [R(int) = 0.1243]	
Refined parameters	352	
Final R indices	$R_1 = 0.0612$, $wR_2 = 0.1418$	
GooF	1.159	
Weighting scheme $P = (F_o^2+2F_c^2)/3$	$w = 1/[\sigma^2(F_o^2)+(0.0785P)^2]$	

Table 3.4.4. Selected bond lengths and bond angles of $[(H_2O)Cl_4Os{\equiv}N\text{-}IrClCp^*(Ph_3As)]\cdot(H_2O)$

Bond Lengths [pm]			
Os-N	167.7(10)	Ir-C(1)	220.9(14)
Ir-N	191.2(11)	Ir-C(2)	220.1(13)
Os-Cl(1)	236.2(3)	Ir-C(3)	224.1(13)
Os-Cl(2)	235.8(3)	Ir-C(4)	222.5(12)
Os-Cl(3)	234.1(3)	Ir-C(5)	222.3(12)
Os-Cl(4)	233.3(4)	Ir-Cl(5)	239.1(3)
Os-O(1)	221.8(8)	Ir-As	245.9(14)
C(1)-C(2)	143(2)	C(4)-C(5)	146(2)
C(2)-C(3)	145(2)	C(5)-C(1)	141(2)
C(3)-C(4)	140(2)		

Bond Angles [º]			
Os-N-Ir	173.6(7)	As-Ir-C(1)	150.3(4)
N-Os-Cl(1)	94.7(4)	As-Ir-C(2)	112.5(4)
N-Os-Cl(2)	99.4(4)	As-Ir-C(3)	93.7(4)
N-Os-Cl(3)	98.2(4)	As-Ir-C(4)	109.7(4)
N-Os-Cl(4)	96.9(4)	As-Ir-C(5)	147.6(4)
N-Os-O(1)	177.3(5)	N-Ir-As	95.6(3)
O(1)-Os-Cl(1)	84.1(3)	N-Ir-C(1)	94.0(5)
O(1)-Os-Cl(2)	83.1(3)	N-Ir-C(2)	104.9(4)
O(1)-Os-Cl(3)	83.0(3)	N-Ir-C(3)	141.7(5)
O(1)-Os-Cl(4)	80.9(3)	N-Ir-C(4)	154.5(5)
Cl(1)-Os-Cl(2)	91.97(12)	N-Ir-C(5)	116.7(5)
Cl(2)-Os-Cl(3)	85.57(12)	N-Ir-Cl(5)	91.4(3)
Cl(3)-Os-Cl(4)	91.93(14)	Cl(5)-Ir-C(1)	122.2(4)
Cl(4)-Os-Cl(1)	86.85(13)	Cl(5)-Ir-C(2)	153.8(3)
Cl(1)-Os-Cl(3)	167.05(12)	Cl(5)-Ir-C(3)	95.6(3)
Cl(2)-Os-Cl(4)	164.01(12)	Cl(5)-Ir-C(4)	126.3(4)
As-Ir-Cl(5)	85.61(9)	Cl(5)-Ir-C(5)	90.8(4)

Bond Angles [º]			
C(1)-Ir-C(2)	37.8(5)	C(3)-Ir-C(5)	63.0(5)
C(1)-Ir-C(3)	62.3(5)	C(4)-Ir-C(5)	38.4(5)
C(1)-Ir-C(4)	62.3(5)	C(1)-C(2)-C(3)	106.4(11)
C(1)-Ir-C(5)	37.2(5)	C(2)-C(3)-C(4)	108.3(13)
C(2)-Ir-C(3)	38.0(5)	C(3)-C(4)-C(5)	108.9(13)
C(2)-Ir-C(4)	62.9(5)	C(4)-C(5)-C(1)	105.8(14)
C(2)-Ir-C(5)	63.6(5)	C(5)-C(1)-C(2)	110.4(12)
C(3)-Ir-C(4)	36.6(5)		

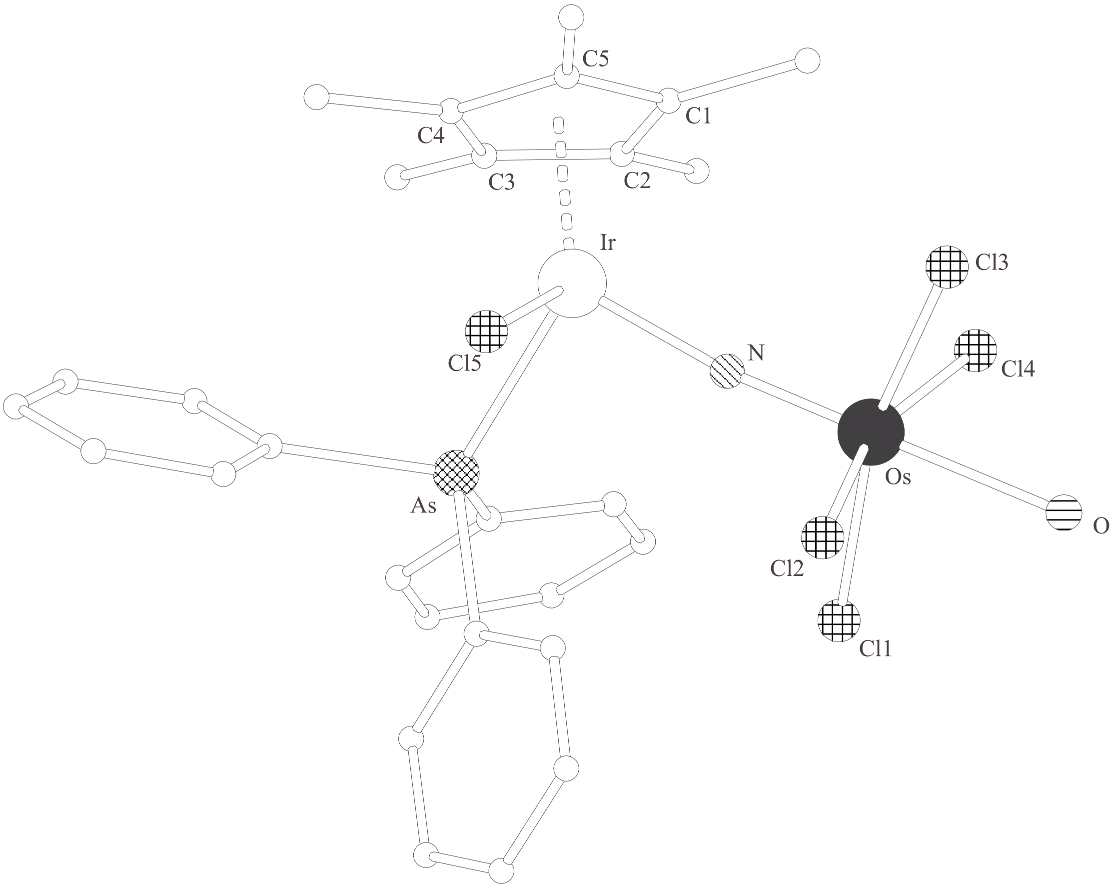

Figure 3.4.1. Crystal structure of **$[(H_2O)Cl_4Os\equiv N\text{-}IrClCp^*(Ph_3As)]\cdot(H_2O)$**; the hydrogen atoms have been excluded for clarity.

3.4.4. Discussion and Structure of

$[(H_2O)Cl_4Os\equiv N\text{-}IrClCp^*(Ph_3As)]\cdot(H_2O)$

The nitrido complex, $[(H_2O)Cl_4Os\equiv N\text{-}IrClCp^*(Ph_3As)]\cdot(H_2O)$, crystallises in the monoclinic space group Cm, with 4 molecules per unit cell. The nitrido complex $[(Ph_3As)_2Cl_3Os\equiv N]$ coordinates through the terminal nitrido ligand to the IrClCp* fragment by forming an almost linear nitrido bridge with an Os-N-Ir bond angle of 173.6(7)º, with an Os-N-bond length of 167.7(10) pm, which corresponds to an Os-N-triple bond, and an Ir-N-bond length of 191.2(11) pm. The π-component of the Ir-N-bond also affects the distance between the Cp* ring and the iridium centre, with a longer Ir-C(4)-distance of 224.1(13) pm in the *trans*-position with respect to the Ir-N-bond, when compared to the Ir-C(1)-distance of 220.9(14) pm in the *cis*-position.

The octahedral coordinated osmium atom is made up of a plane consisting of four chlorine atoms, with the other two positions occupied by the nitrido ligand, and the coordinated water molecule. Of the two triphenyl-arsane ligands present in the starting material, one migrates to the iridium atom, and the other is not accounted for, presumably taking part in a coupled reaction (see above) to form a by-product. The two octahedral positions vacated by the triphenyl-arsane ligands are occupied by a chlorine atom, which has migrated from the iridium atom, and the coordinated water molecule, which is essential for the crystallisation of this complex. This is similar to the finding by S. Schwarz [12] where the complex $[\{(L)Cl_4Re\equiv N\}_2PtCl_2]^{2-}$ required a coordinating molecule in *trans*-position (H_2O or NMP) to the nitrido function, for the crystallization process to occur. The chlorine atoms about the osmium atom have also undergone a rearrangement, with the chloro ligand in *trans*-position in the starting material occupying an equatorial position in the nitrido complex $[(H_2O)Cl_4Os\equiv N\text{-}IrClCp^*(Ph_3As)]\cdot(H_2O)$.

3.4.5. Magnetic Properties of [$(H_2O)Cl_4Os\equiv N\text{-}IrClCp^*(Ph_3As)$].($H_2O$)

In the nitrido complex, [$(H_2O)Cl_4Os\equiv N\text{-}IrClCp^*(Ph_3As)$].($H_2O$), both the osmium and the iridium atoms occupy octahedral sites, and the complex exhibits temperature independent paramagnetism, with a molar susceptibility of $2.7\cdot10^{-3}$ emu/mol at 295 K. This confirms that although there was a transfer of a chlorine atom from the iridium to the osmium atom, a corresponding change in the oxidation state of the metals did not occur, which would have been accompanied by the temperature dependent paramagnetism associated with two unpaired electrons.

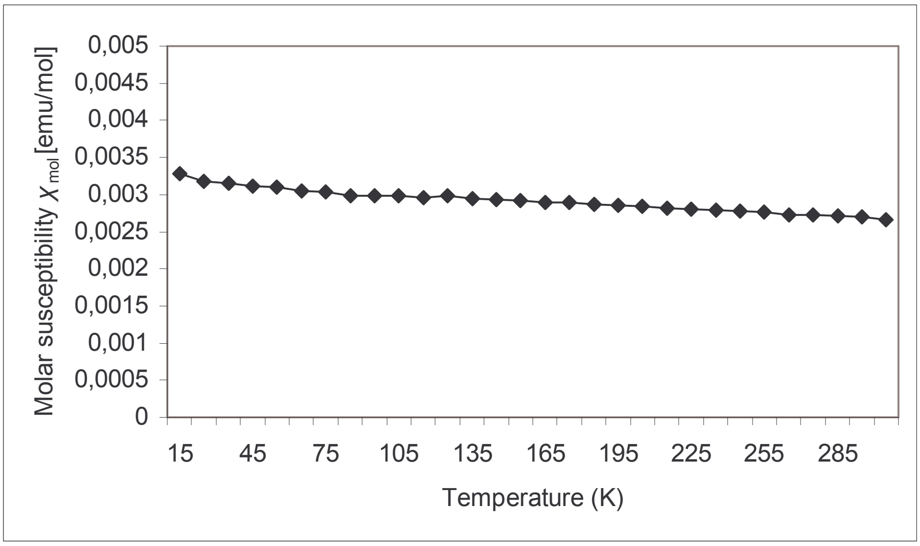

Figure 3.4.2. Magnetic susceptibility χ_{mol} of **[$(H_2O)Cl_4Os\equiv N\text{-}IrClCp^*(Ph_3As)$]•($H_2O$)** as a function of temperature (K).

3.5. $[(Ph_3Sb)_2Cl_3Os{\equiv}N\text{-}IrCl(COD)]$

3.5.1. General

The nitrido ligand of $[(Ph_3Sb)_2OsNCl_3]$ reacts with the dimeric iridium compound $[Ir(\mu\text{-}Cl)(COD)]_2$ in a similar fashion to the arsane analogue **[3.3.]**, with the strongly basic nitrido ligand of $[(Ph_3Sb)_2OsNCl_3]$ breaking the chloro bridge of the iridium complex to form an asymmetrically bridged nitrido complex. Although the reaction mechanism is obviously similar to the arsane complex described previously, the product is subtly different; the stibane ligands are mutually *cis*- to one another, as opposed to the analogous arsane complex, $[(Ph_3As)_2Cl_3Os{\equiv}N\text{-}IrCl(COD)]$, where the arsane ligands are mutually *trans*- to one and other.

3.5.2. Spectroscopic Analysis

In the IR-spectrum of $[(Ph_3Sb)_2Cl_3Os{\equiv}N\text{-}IrCl(COD)]$ the Os≡N absorption is observed at 1066 cm^{-1}. The Os-Cl stretch occurs at 314 cm^{-1}. The Os≡N absorption occurs in the same area as the uncoordinated Os≡N stretch of $[(Ph_3Sb)_2Cl_3OsN]$.

Table 3.5.1. Selected IR vibrations of $[(Ph_3Sb)_2Cl_3Os{\equiv}N\text{-}IrCl(COD)]$

Vibration	υ(Os≡N)	υ(Os-Cl)
$[(Ph_3Sb)_2Cl_3OsN]$	1065 st	338 st
$[(Ph_3Sb)_2Cl_3Os{\equiv}N\text{-}IrCl(COD)]$	1066 st	314 w
$[(Ph_3As)_2Cl_3Os{\equiv}N\text{-}IrCl(COD)]$	1063 w	334 w

In the FAB(+) mass spectrum, the following fragments from the complex [$(Ph_3Sb)_2Cl_3Os{\equiv}N$-IrCl(COD)] were identified. No bridged complex fragments were found.

Table 3.5.2. Identifiable peaks from the FAB(+) mass spectrum of [$(Ph_3Sb\,_2Cl_3Os{\equiv}N$-IrCl(COD)]

Peak	Intensity	Fragment
887	5	$[(Ph_3As)_2Cl_2OsN]^+$
579	5	$[(Ph_3As)Cl_2OsN]^+$

3.5.3. Structural Analysis of [$(Ph_3Sb)_2Cl_3Os{\equiv}N$-IrCl(COD)]

Table 3.5.3. Details from the structural analysis of [$(Ph_3Sb_2Cl_3Os{\equiv}N$-IrCl(COD)]

Empirical formula	$C_{44}H_{42}Cl_4NOsIrSb_2$	
Formula weight [g/mol]	1352.49	
Crystal system	triclinic	
Space group	$P\bar{1}$	
Unit cell dimensions [pm] [º]	a = 1078.41(14)	α = 101.192(9)
	b = 1172.31(12)	β = 92.703(10)
	c = 1696.72(19)	γ = 92.614(10)
Volume [pm^3]	$2100.6(4)\cdot10^6$	
Z	2	
Calculated density [g/cm^3]	2.138	
F(000)	1272	
Absorption coefficient [mm^{-1}]	7.732	
Radiation	MoK_α	
Temperature [K]	173	
Crystal size [mm^3]	0.30 x 0.10 x 0.05	
Crystal description	brown platelets	
Diffractometer	STOE, IPDS	
Theta range θ_{max}[º]	29	
Index ranges h, k, l	-14 → 14, -15 → 16, -23 → 23	
Reflections collected	19098	
Independent reflections	10343 [R(int) = 0.0725]	
Decay	0	
Refined parameters	480	
Final R indices	R_1 = 0.0681, wR_2 = 0.1374	
GooF	1.152	
Weighting scheme $P = (F_o^2+2F_c^2)/3$	$w = 1/[\sigma^2(F_o^2)+(0.0448P)^2+38.7726P]$	

Table 3.5.4. Selected bond lengths and bond angles of $[(Ph_3Sb\ _2Cl_3Os{\equiv}N\text{-}IrCl(COD)]$

	Bond Lengths [pm]		
Os-N	171.9(11)	Ir-Cl(4)	232.8(3)
Ir-N	182.0(11)	Os-Cl(1)	239.5(3)
Ir-C(1)	228.4(15)	Os-Cl(2)	238.5(3)
Ir-C(2)	226.6(15)	Os-Cl(3)	246.6(3)
Ir-C(5)	218.0(11)	Os-Sb(1)	263.78(10)
Ir-C(6)	213.5(12)	Os-Sb(2)	264.26(9)
C(1)-C(2)	137(3)	C(5)-C(6)	148(2)
C(2)-C(3)	147(2)	C(6)-C(7)	151(2)
C(3)-C(4)	152(2)	C(7)-C(8)	151(3)
C(4)-C(5)	148(2)	C(1)-C(8)	151(2)

	Bond Angles [º]		
Os-N-Ir	175.6(7)	N-Ir-Cl(4)	93.6(3)
N-Os-Cl(1)	96.0(4)	N-Ir-C(1)	172.4(6)
N-Os-Cl(2)	101.3(4)	N-Ir-C(2)	151.2(6)
N-Os-Cl(3)	167.1(3)	N-Ir-C(5)	91.0(5)
N-Os-Sb(1)	93.5(4)	N-Ir-C(6)	92.8(5)
N-Os-Sb(2)	88.0(4)	Cl(4)-Ir-C(1)	90.1(4)
Cl(1)-Os-Cl(2)	86.92(12)	Cl(4)-Ir-C(2)	91.0(4)
C1(1)-Os-C1(3)	91.99(11)	Cl(4)-Ir-C(5)	167.0(4)
Cl(1)-Os-Sb(1)	82.30(8)	Cl(4)-Ir-C(6)	151.4(5)
Cl(1)-Os-Sb(2)	169.67(9)	C(1)-Ir-C(2)	35.1(7)
C1(2)-Os-Cl(3)	89.19(12)	C(1)-Ir-C(5)	86.8(6)
Cl(2)-Os-Sb(1)	162.55(9)	C(1)-Ir-C(6)	80.9(6)
Cl(2)-Os-Sb(2)	82.94(9)	C(2)-Ir-C(5)	79.2(6)
Cl(3)-Os-Sb(1)	77.56(8)	C(2)-Ir-C(6)	96.9(6)
Cl(3)-Os-Sb(2)	85.91(8)	C(5)-Ir-C(6)	40.0(6)
Sb(1)-Os -Sb(2)	107.04(3)		

Bond Angles [º]			
C(1)-C(2)-C(3)	125.4(15)	C(5)-C(6)-C(7)	122.4(14)
C(2)-C(3)-C(4)	114.5(15)	C(6)-C(7)-C(8)	117.0(14)
C(3)-C(4)-C(5)	113.0(12)	C(7)-C(8)-C(1)	112.6(13)
C(4)-C(5)-C(6)	124.3(14)	C(8)-C(1)-C(2)	126.5(17)

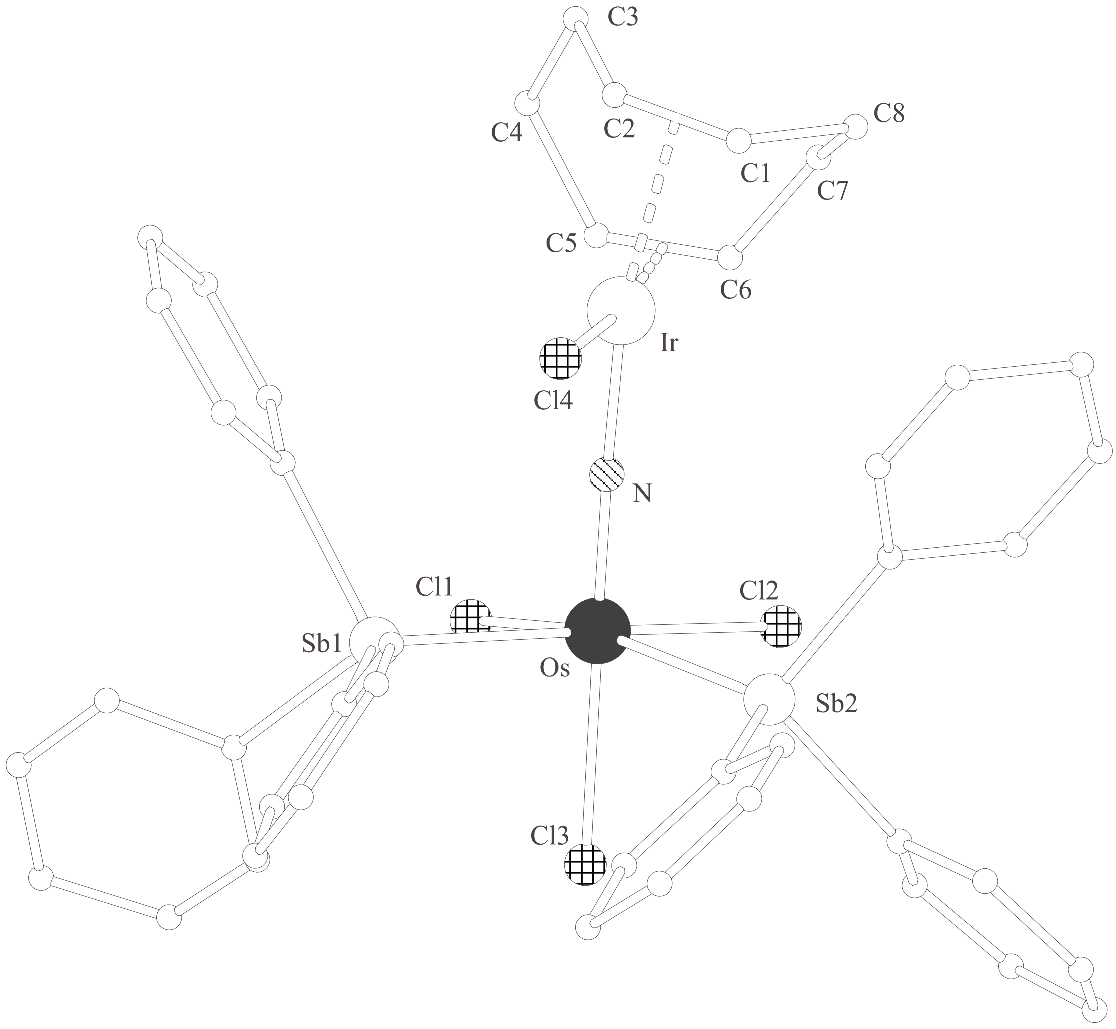

Figure 3.5.1. Crystal structure of **$[(\mathrm{Ph_3Sb})_2\mathrm{Cl_3Os{\equiv}N\text{-}IrCl(COD)}]$**; the hydrogen atoms have been excluded for clarity.

3.5.4. Discussion and Structure of [$(Ph_3Sb)_2Cl_3Os{\equiv}N$-IrCl(COD)]

The dinuclear complex, [$(Ph_3Sb)_2Cl_3Os{\equiv}N$-IrCl(COD)], crystallises in the triclinic space group $P\bar{1}$, with two molecules per unit cell. The nitrido complex [$(Ph_3Sb)_2Cl_3Os{\equiv}N$] coordinates to the IrCl(COD) fragment by forming a nitrido bridge. The monovalent iridium atom attains quadratic planar geometry, with both π-bonds to the cycloocatdiene ligand in *cis*-position. The octahedrally coordinated osmium atom has three facially arranged chlorine ligands, with two stibane ligands mutually *cis*- to one another, and in *cis*-position to the nitrido bridge. This *cis*-arrangement of the stibane ligands contrasts to the *trans*- arrangement of the starting material [$(Ph_3Sb)_2Cl_3Os{\equiv}N$] suggested by Griffith et al. [6], and confirmed by our preliminary X-ray analysis of [$(Ph_3Sb)_2Cl_3Os{\equiv}N$] crystals.

The nitrido bridge is almost linear with an Os-N-Ir angle of 175.6(7)º. The Os-N-bond length at 171.9(11) pm corresponds to an Os-N triple bond. A similar Os-N-bond length was found in [$(Ph_3Sb)_2Cl_3Os{\equiv}N$-RhCl(COD)], the rhodium analogue to this compound, with a Os-N-bond length of 168.3(7) pm [9]. The Ir-N-bond length at 182.0(11) pm is much shorter than the sum of the covalent radii of the two atoms as given by Pauling [10]. This is due to a π-component to the bond, which also influences the Ir-C-bond lengths to the cyclooctadiene fragment, with the Ir-C-bond lengths in the *trans*-position to the nitrido bridge, 228.4(15) and 226.6(15) pm, being distinctly longer than those in the *cis*-position 213.5(12) and 218.0(11) pm. The difference in bond lengths between the chlorine atoms in *trans*- and *cis*- positions with respect to the nitrido ligand is about 7 pm.

3.5.5. Magnetic Properties of [$(Ph_3Sb)_2Cl_3Os\equiv N$-IrCl(COD)]

Due to the +VI oxidation state of the octahedrally coordinated osmium, and the quadratic planar coordinated iridium(I), the [$(Ph_3Sb)_2Cl_3Os\equiv N$-IrCl(COD)] complex was expected to be diamagnetic. The complex actually exhibits temperature independent paramagnetism, with a molar susceptibility of $1.57 \cdot 10^{-5}$ emu/mol at 295 K.

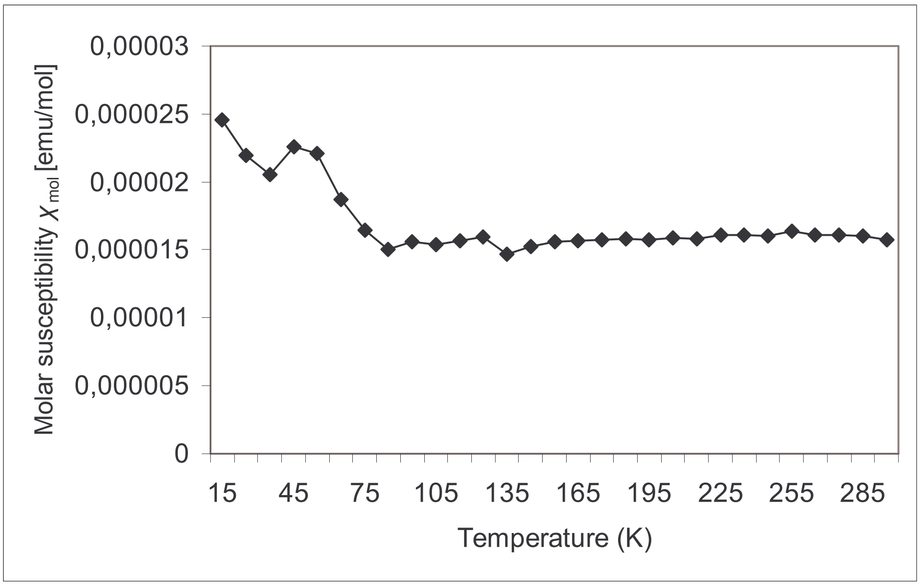

Figure 3.5.2. Magnetic susceptibility χ_{mol} of **[$(Ph_3Sb)_2Cl_3Os\equiv N$-IrCl(COD)]** as a function of temperature (K).

3.6. [$(Ph_3Sb)Cl_4Os$≡N-IrClCp*(Ph_3Sb)]

3.6.1. General

The nitrido ligand of [$(Ph_3Sb)_2OsNCl_3$] reacts with the dimeric iridium compound [$IrCl_2Cp^*]_2$, with the strongly basic nitrido ligand of [$(Ph_3Sb)_2OsNCl_3$] breaking the chloro bridge of the iridium complex, to form a dinuclear nitrido complex [$(Ph_3Sb)Cl_4Os$≡N-IrClCp*(Ph_3Sb)], with an almost symmetrical nitrido bridge. Unexpectedly, one of the stibane ligands on the osmium swaps places with a chloro ligand on the iridium atom which results in a nitrido complex with two stibane ligands, one coordinated to each metal atom.

The reaction only proceeded when the reaction mixture was refluxed; suggesting that at lower temperatures, the triphenyl-stibane ligands on the osmium atom are too tightly bound to migrate to the iridium atom, and therefore the bridged complex cannot be formed.

3.6.2. Spectroscopic Analysis

In the IR-spectrum of [$(Ph_3Sb)Cl_4Os$≡N-IrClCp*(Ph_3Sb)], the Os≡N absorption is observed at 1019 cm^{-1}. The Os-Cl stretch occurs at 313 cm^{-1}.

Table 3.6.1. Selected IR vibrations of [$(Ph_3Sb)Cl_4Os$≡N-IrClCp*(Ph_3Sb)]

Vibration	υ(Os≡N)	υ(Os-Cl)
[PPh_4][$OsNCl_4$] [11]	1123 st	338 st
[$(Ph_3Sb)Cl_4Os$≡N-IrClCp*(Ph_3Sb)]	1019 st	313 w

In the FAB(+) mass spectrum the following fragments from the complex [$(Ph_3Sb)Cl_4Os\equiv N$-IrClCp*(Ph_3Sb)] were identified. No bridged complex fragments were found.

Table 3.6.2. Identifiable peaks from the FAB(+) mass spectrum of [$(Ph_3Sb)Cl_4Os\equiv N$-IrClCp*(Ph_3Sb)]

Peak	Intensity	Fragment
714	50	$[(Ph_3Sb)IrClCp^*]^+$
601	15	$[(Ph_3Sb)OsNCl]^+$
362	70	$[IrClCp^*]^+$
327	50	$[IrCp^*]^+$

3.6.3. Structural Analysis of [$(Ph_3Sb)Cl_4Os{\equiv}N\text{-}IrClCp^*(Ph_3Sb)$]

Table 3.6.3. Details from the structural analysis of [$(Ph_3Sb)Cl_4Os{\equiv}N\text{-}IrClCp^*(Ph_3Sb)$]

Empirical formula	$C_{46}H_{45}Cl_5NOsIrSb_2$	
Formula weight [g/mol]	1414.98	
Crystal system	triclinic	
Space group	$P\bar{1}$	
Unit cell dimensions [pm] [º]	a = 1023.3(3)	α = 74.6(2)
	b = 1476.2(3)	β = 73.84(2)
	c = 1872.5(6)	γ = 76.191(19)
Volume [pm^3]	$2577.7(12)\cdot10^6$	
Z	2	
Calculated density [g/cm^3]	1.823	
F(000)	1336	
Absorption coefficient [mm^{-1}]	6.355	
Radiation	MoK_α	
Temperature [K]	173	
Crystal size [mm^3]	0.20 x 0.02 x 0.01	
Crystal description	brown platelets	
Diffractometer	STOE, IPDS	
Theta range θ_{max}[º]	23.26	
Index ranges h, k, l	-11 → 10, -15 → 16, -20 → 20	
Reflections collected	9948	
Independent reflections	6399 [R(int) = 0.1381]	
Decay	0	
Refined parameters	225	
Final R indices	$R_1 = 0.1614$, $wR_2 = 0.3457$	
GooF	1.080	
Weighting scheme $P = (F_o^2+2F_c^2)/3$	$w = 1/[\sigma^2(F_o^2)+(0.0922P)^2+ 541.9697P]$	

Table 3.6.4. Selected bond lengths and bond angles of [$(Ph_3Sb)Cl_4Os{\equiv}N\text{-}IrClCp^*(Ph_3Sb)$]

	Bond Lengths [pm]		
Os-N	174(4)	Ir-C(1)	210(5)
Ir-N	187(4)	Ir-C(2)	222(6)
Os-Cl(1)	237.2(13)	Ir-C(3)	223(3)
Os-Cl(2)	235.2(14)	Ir-C(4)	231(6)
Os-Cl(3)	237.4(16)	Ir-C(5)	216(5)
Os-Cl(4)	244.6(16)	Ir-Cl(5)	238.8(13)
Os-Sb(1)	261.9(4)	Ir-Sb(2)	260.6(4)
C(1)-C(2)	127(8)	C(4)-C(5)	149(7)
C(2)-C(3)	133(7)	C(5)-C(1)	145(7)
C(3)-C(4)	145(6)		

	Bond Angles [º]		
Os-N-Ir	173(3)	Sb(2)-Ir-C(1)	154.1(14)
N-Os-Cl(1)	94.7(15)	Sb(2)-Ir-C(2)	143.5(17)
N-Os-Cl(2)	92.0(15)	Sb(2)-Ir-C(3)	108.9(8)
N-Os-Cl(3)	92.4(15)	Sb(2)-Ir-C(4)	92.2(13)
N-Os-Cl(4)	176.8(15)	Sb(2)-Ir-C(5)	114.5(12)
N-Os-Sb(1)	101.9(14)	N-Ir-Sb(2)	91.1(13)
Sb(1)-Os-Cl(1)	82.2(3)	N-Ir-C(1)	99(2)
Sb(1)-Os-Cl(2)	164.8(4)	N-Ir-C(2)	125(2)
Sb(1)-Os-Cl(3)	96.3(4)	N-Ir-C(3)	159.9(16)
Sb(1)-Os-Cl(4)	80.8(4)	N-Ir-C(4)	143.3(18)
Cl(1)-Os-Cl(2)	90.9(5)	N-Ir-C(5)	108.1(18)
Cl(2)-Os-Cl(3)	88.9(5)	N-Ir-Cl(5)	91.1(14)
Cl(3)-Os-Cl(4)	85.7(6)	Cl(5)-Ir-C(1)	120.8(14)
Cl(4)-Os-Cl(1)	87.2(5)	Cl(5)-Ir-C(2)	96.1(17)
Cl(1)-Os-Cl(3)	172.9(5)	Cl(5)-Ir-C(3)	93.9(9)
Cl(2)-Os-Cl(4)	85.4(5)	Cl(5)-Ir-C(4)	125.5(13)
Sb(2)-Ir-Cl(5)	82.6(3)	Cl(5)-Ir-C(5)	153.3(12)

Bond Angles [º]			
C(1)-Ir-C(2)	34(2)	C(3)-Ir-C(5)	61.9(14)
C(1)-Ir-C(3)	62.0(16)	C(4)-Ir-C(5)	38.9(17)
C(1)-Ir-C(4)	66(2)	C(1)-C(2)-C(3)	119(6)
C(1)-Ir-C(5)	39.7(18)	C(2)-C(3)-C(4)	107(4)
C(2)-Ir-C(3)	34.6(19)	C(3)-C(4)-C(5)	100(4)
C(2)-Ir-C(4)	59(2)	C(4)-C(5)-C(1)	110(4)
C(2)-Ir-C(5)	58(2)	C(5)-C(1)-C(2)	102(5)
C(3)-Ir-C(4)	37.2(15)		

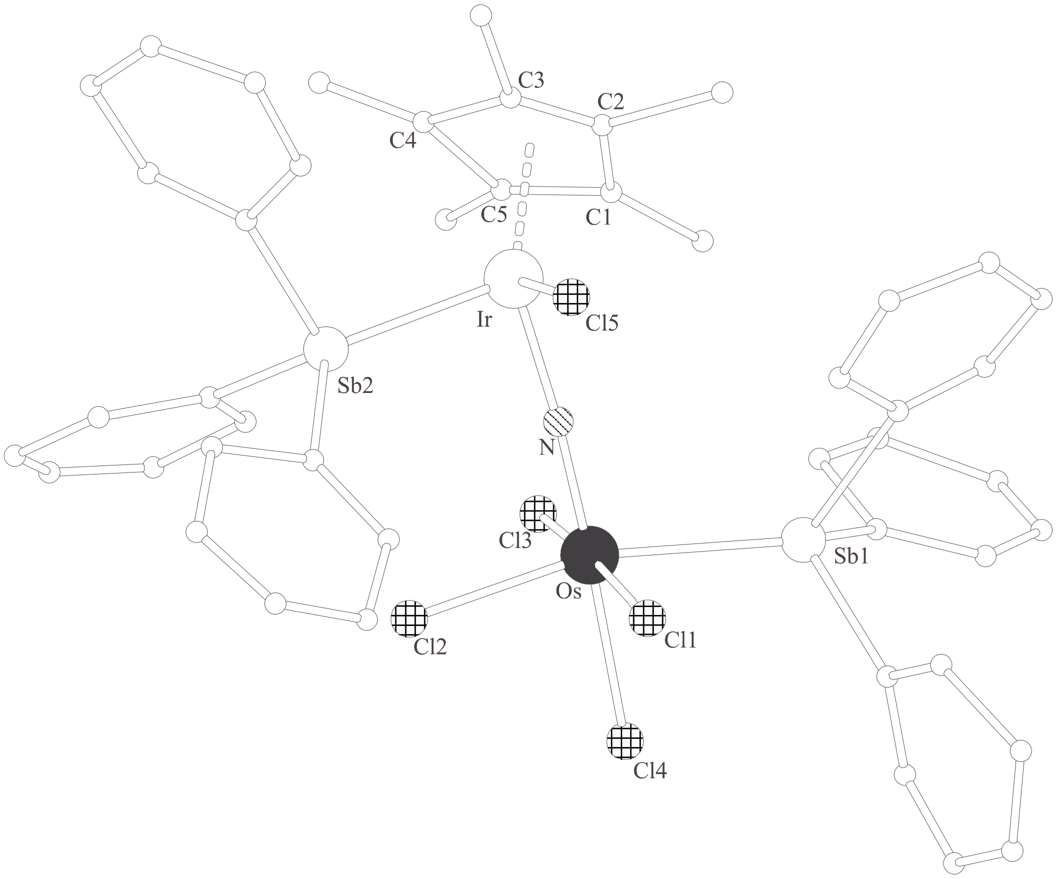

Figure 3.6.1. Crystal structure of **$[(Ph_3Sb)Cl_4Os\equiv N\text{-}IrClCp^*(Ph_3Sb)]$**; the hydrogen atoms have been excluded for clarity.

3.6.4. Discussion and Structure of [$(Ph_3Sb)Cl_4Os\equiv N\text{-}IrClCp^*(Ph_3Sb)$]

The dinuclear nitrido complex, [$(Ph_3Sb)Cl_4Os\equiv N\text{-}IrClCp^*(Ph_3Sb)$], crystallises in the triclinic space group $P\bar{1}$, with two molecules per unit cell. The crystals were unfortunately very thin, clumped together platelets, making it impossible to isolate a single crystal. The X-ray structural analysis was therefore difficult, and this is reflected in the rather high R_1 and R_2 values.

The octahedrally coordinated osmium atom has four chloro ligands, three of which share an equatorial plane with the triphenyl-stibane ligand, with the fourth chloro ligand is in *trans*-position to the nitrido bridge. The iridium atom is in an octahedral environment, with the Cp* ligand occupying three facially arranged coordination sites, leaving the other three sites free for the triphenyl-stibane, chlorine and the Ir-N-bond.

The nitrido bridge is almost linear with an Os-N-Ir angle of 173(3)º. The Os-N-bond length at 174(4) pm indicates an Os-N triple bond. The Ir-N-bond length of 187(4) pm is similar in length to the 191.2(11) pm Ir-N-bond length in the complex [$(H_2O)Cl_4Os\equiv N\text{-}IrClCp^*(Ph_3As)$]•($H_2O$). The π-component of the Ir-N-bond also affects the distance between the Cp* ring and the iridium atom, with the longest Ir-C-distance of 231(6) pm in the *trans*-position with respect to the Ir-N-bond, and the shortest Ir-C-distance of 210(5) pm in *cis*-position. The Os-Cl-bond lengths also exhibit the influence of the nitrido functional group on the complex geometry, with *trans*- Os-Cl-bond length of 244.6(16) pm being on average about 7 pm longer than the Os-Cl- bond lengths in axial positions.

3.6.5. Magnetic Properties of [(Ph$_3$Sb)Cl$_4$Os≡N-IrClCp*(Ph$_3$Sb)]

The nitrido complex, [(Ph$_3$Sb)Cl$_4$Os≡N-IrClCp*(Ph$_3$Sb)], exhibits temperature independent paramagentism; the molar susceptibility of [(Ph$_3$Sb)Cl$_4$Os≡N-IrClCp*(Ph$_3$Sb)] at 295 K is $2.27 \cdot 10^{-3}$ emu/mol.

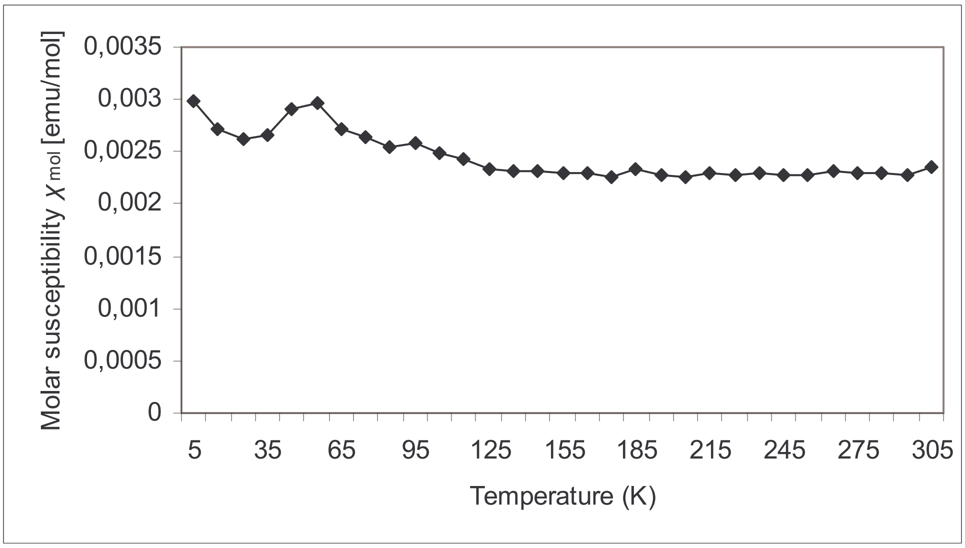

Figure 3.6.2. Magnetic susceptibility χ_{mol} of **[(Ph$_3$Sb)Cl$_4$Os≡N-IrClCp*(Ph$_3$Sb)]** as a function of temperature (K).

3.7. [(Ph$_3$As)RhCl$_2$Cp*]

3.7.1. General

The nitrido complex [(Ph$_3$As)$_2$OsNCl$_3$] reacts with the dimeric rhodium compound [RhCl$_2$(Cp*)]$_2$, to form the rhodium arsane compound, [(Ph$_3$As)RhCl$_2$Cp*]. Presumably, analogue to the previously described reactions, the nitrido ligand of the [(Ph$_3$As)$_2$OsNCl$_3$] breaks the chloro bridge but, instead of affording the expected osmium-rhodium nitrido complex, a by product is formed. Obviously, a tandem reaction occurs, similar to the reaction described in the previous section;

$$\left[\left(\mathrm{Ph_3As}\right)_2\mathrm{OsNCl_3}\right]+\left[\mathrm{RhCl_2}\left(\mathrm{Cp}*\right)\right]_2\longrightarrow$$

$$\left[\mathrm{Cl_4Os}\equiv\mathrm{N}-\mathrm{RhClCp}*\left(\mathrm{Ph_3As}\right)\right]+\left[\left(\mathrm{Ph_3As}\right)\mathrm{RhCl_2Cp}*\right]$$

The difference being that in this case the by-product was isolated and structurally characterised, as opposed to the previous section, where the nitrido complex was isolated.

3.7.2. Structural Analysis of [(Ph_3As)$RhCl_2Cp^*$]

Table 3.7.1. Details from the structural analysis of [(Ph_3As)$RhCl_2Cp^*$]

Empirical formula	$C_{28}H_{30}AsCl_2Rh$	
Formula weight [g/mol]	615.25	
Crystal system	monoclinic	
Space group	Cm	
Unit cell dimensions [pm] [º]	a = 8608.6(4)	$\alpha = 90$
	b = 32276.4(18)	$\beta = 90.372(4)$
	c = 18257.9(9)	$\gamma = 90$
Volume [pm^3]	$5072.9(4) \cdot 10^6$	
Z	8	
Calculated density [g/cm^3]	1.611	
F(000)	2480	
Absorption coefficient [mm^{-1}]	2.193	
Radiation	MoK_α	
Temperature [K]	223	
Crystal size [mm^3]	0.80 x 0.05 x 0.05	
Crystal description	red platelets	
Diffractometer	STOE, IPDS	
Theta range θ_{max}[º]	31.22	
Index ranges h, k, l	-11→ 11, -45 → 26, -22 → 24	
Reflections collected	23279	
Independent reflections	13321[R(int) = 0.0501]	
Refined parameters	577	
Final R indices	$R_1 = 0.0690$, $wR_2 = 0.0997$	
GooF	1.098	
Weighting scheme $P = (F_o^2+2F_c^2)/3$	$w = 1/[\sigma^2(F_o^2)+(0.0144P)^2 + 26.0410P]$	

Table 3.7.2. Selected bond lengths and bond angles of [(Ph$_3$As)RhCl$_2$Cp*]

Bond Lengths [pm]			
Rh(1)-As(1)	244.94(7)	As(1)-C(11)	194.6(6)
Rh(1)-Cl(11)	240.96(15)	As(1)-C(21)	194.3(6)
Rh(1)-Cl(12)	240.04(14)	As(1)-C(31)	194.3(6)
Rh(1)-C(1)	220.2(6)	C(1)-C(2)	140.6(8)
Rh(1)-C(2)	219.5(5)	C(2)-C(3)	145.5(8)
Rh(1)-C(3)	215.4(6)	C(3)-C(4)	142.9(8)
Rh(1)-C(4)	217.5(6)	C(4)-C(5)	143.8(8)
Rh(1)-C(5)	215.7(6)	C(1)-C(5)	144.5(8)

Bond Angles [º]			
Cl(11)-Rh(1)-Cl(12)	91.54(6)	Cl(11)-Rh(1)-C(2)	92.34(16)
As(1)-Rh(1)- Cl(11)	86.26(4)	Cl(11)-Rh(1)-C(3)	95.25(17)
As(1)-Rh(1)- Cl(12)	87.26(4)	Cl(11)-Rh(1)-C(4)	129.84(17)
As(1)-Rh(1)- C(1)	151.50(16)	Cl(11)-Rh(1)-C(5)	156.44(16)
As(1)-Rh(1)- C(2)	156.22(15)	Cl(12)-Rh(1)-C(1)	91.64(15)
As(1)-Rh(1)- C(3)	117.35(15)	Cl(12)-Rh(1)-C(2)	116.51(15)
As(1)-Rh(1)- C(4)	98.75(15)	Cl(12)-Rh(1)-C(3)	154.79(16)
As(1)-Rh(1)- C(5)	113.79(15)	Cl(12)-Rh(1)-C(4)	138.32(17)
Cl(11)-Rh(1)-C(1)	122.24(16)	Cl(12)-Rh(1)-C(5)	101.26(16)

Bond Angles [º]			
C(1)-Rh-C(2)	37.3(2)	C(3)- Rh-C(5)	65.1(2)
C(1)-Rh-C(3)	64.3(2)	C(4)- Rh-C(5)	38.8(2)
C(1)-Rh-C(4)	64.1(2)	C(1)-C(2)-C(3)	108.2(5)
C(1)-Rh-C(5)	38.7(2)	C(2)-C(3)-C(4)	107.5(5)
C(2)-Rh-C(3)	39.1(2)	C(3)-C(4)-C(5)	108.1(5)
C(2)-Rh-C(4)	64.3(2)	C(4)-C(5)-C(1)	107.5(5)
C(2)-Rh-C(5)	64.3(2)	C(5)-C(1)-C(2)	108.6(5)
C(3)-Rh-C(4)	38.5(2)		

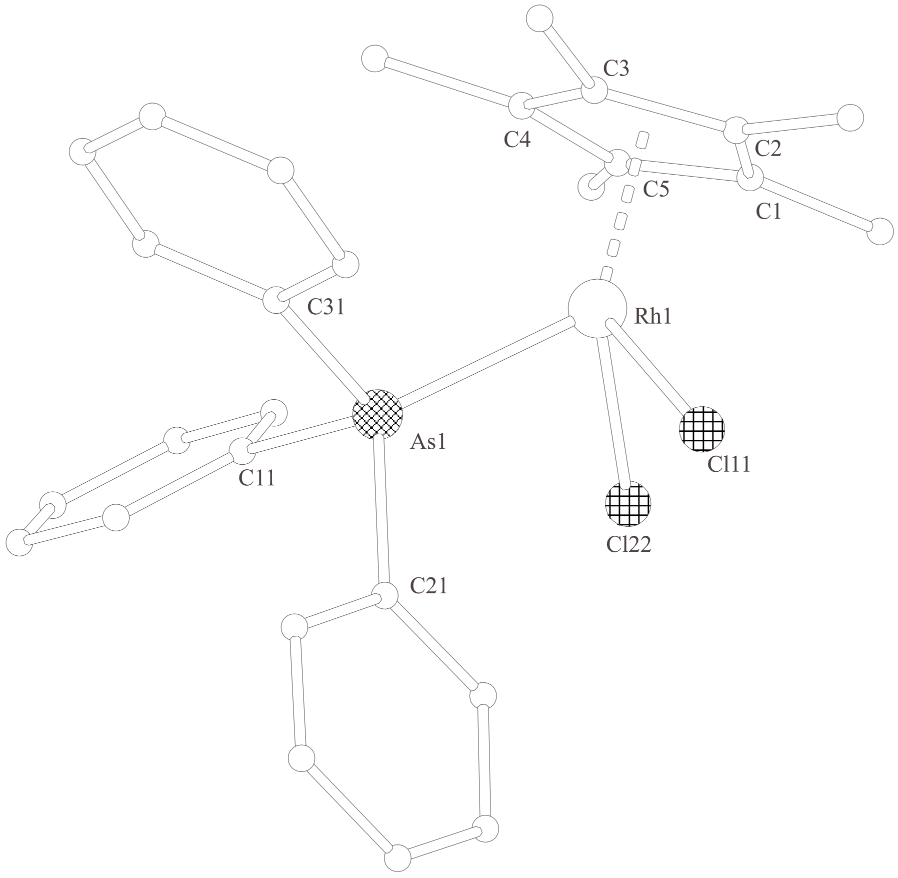

Figure 3.7.1. Crystal structure of **[(Ph$_3$As)RhCl$_2$Cp*]**; the hydrogen atoms have been excluded for clarity.

3.7.3. Discussion and Structure of [(Ph_3As)$RhCl_2Cp$*]

The rhodium-arsane compound [(Ph_3As)$RhCl_2Cp$*], crystallises in the monoclinic space group Cm, with eight molecules per unit cell.

The rhodium atom is in an octahedral environment, with the Cp* ligand occupying three facially arranged coordination sites, leaving the other three sites free for the triphenyl arsane and two chlorine ligands.

The Rh-As bond length of 244.94(7) pm is shorter than the sum of the covalent radii of the two atoms as given by Pauling [10]. The Rh-C(1)-bond length of 220.2(6) pm to the Cp* fragment in *trans*-position to the Rh-As-bond is slightly longer than the Rh-C(4)-bond length of 217.5(6) pm, indicating a π-component to the Rh-As-bond.

4. Experimental Section

4.1. General

All the experimental procedures were carried out in an argon atmosphere using the Schlenk technique. The oxygen and water in the argon were removed by an activated BTS-catalyser and P_4O_{10} on silica gel respectively. The organic solvents were all dried using the usual methods.

4.2. Starting Materials

4.2.1. K[OsO_3N]

K[OsO_3N] was synthesised by dissolving OsO_4 in a concentrated KOH solution; upon addition of NH_4OH the product precipitated out of the solution in the form of yellow crystals [13]. The yield was 80% of the theoretical value.

4.2.2. $(PPh_4)[OsO_3N]$

$(PPh_4)[OsO_3N]$ was formed by adding excess PPh_4Cl to an aquatic $K[OsO_3N]$ solution. The white water insoluble precipitate, $(PPh_4)[OsO_3N]$, was collected and washed with water [14]. 90% yield.

4.2.3. $(PPh_4)[OsNCl_4]$

20 ml of concentrated HCl was added to 2g $(PPh_4)[OsO_3N]$. The pink precipitate, $(PPh_4)[OsNCl_4]$, was collected and washed with a small amount of cold water. 90% yield.

4.2.4. $[(Ph_3As)_2OsNCl_3]$

2g of $(PPh_4)[OsNCl_4]$ was dissolved in 30ml of methanol. An excess of Ph_3As was added to the solution, and the mixture was refluxed for an hour. The mixture was filtered, and the reddish pink precipitate $[(Ph_3As)_2OsNCl_3]$, washed with cold methanol. The product was then dried under vacuum. 80% yield [7].

Elemental analysis of $[(Ph_3As)_2Cl_3OsN]$

[%]	C	H	N
Experimental	46.4	3.2	1.4
Theoretical	46.8	3.3	1.5

4.2.5. $[(Ph_3Sb)_2OsNCl_3]$

2g of $(PPh_4)[OsNCl_4]$ was dissolved in 30ml of methanol. An excess of Ph_3Sb was added to the solution, and the mixture was refluxed for an hour. The mixture was filtered, and the orange precipitate, $[(Ph_3Sb)_2OsNCl_3]$, washed with cold methanol. The product was then dried under vacuum. 80% yield [7].

Elemental analysis of $[(Ph_3Sb)_2Cl_3OsN]$

[%]	C	H	N
Experimental	42.4	2.6	1.3
Theoretical	42.5	3.0	1.4

4.2.6. Purchased Chemicals

[μ-ClIr(COD)]$_2$ (97%), [μ-ClIrClCp*]$_2$ (96%) and [μ-ClRhClCp*]$_2$ (97%) were purchased from Sigam-Aldrich Chemicals. OsO_4 (99.9%) was purchased from Chempur.

4.3. Synthesis of Complexes

4.3.1. $[(Ph_3As)_2Cl_3Os\equiv N\text{-}RhCl(COD)]$

50 mg of $[(Ph_3As)_2OsNCl_3]$ (0.054mmol) was dissolved in 5ml of CH_2Cl_2, 13 mg of [μ-ClRh(COD)]$_2$ (0.027mmol) was added to the pink solution, and an immediate colour change to an dark green was observed. The solution was stirred for an hour, and then a layer of n-hexane was carefully added. Olive-brown $[(Ph_3As)_2Cl_3Os\equiv N\text{-}RhCl(COD)]$ crystals formed after a few days. Yield 70%

Elemental analysis of $[(Ph_3As)_2Cl_3Os\equiv N\text{-}RhCl(COD)]$

[%]	C	H	N
Experimental	43.5	3.6	1.2
Theoretical	45.2	3.6	1.2

4.3.2. [$(Ph_3As)_2Cl_3Os$≡N-IrCl(COD)]

50 mg of [$(Ph_3As)_2OsNCl_3$] (0.054mmol) was dissolved in 5ml of CH_2Cl_2, 16 mg of [μ-ClIr(COD)]$_2$ (0.027mmol) was added to the pink solution, and an immediate colour change to dark olive-green was observed. The solution was stirred for an hour, and then a layer of n-hexane was carefully added. Olive brown [$(Ph_3As)_2Cl_3Os$≡N-IrCl(COD)] crystals formed after 2 days. Yield 70%

Elemental analysis of [$(Ph_3As)_2Cl_3Os$≡N-IrCl(COD)]

[%]	C	H	N
Experimental	40.3	2.8	1.1
Theoretical	42.0	3.3	1.1

4.3.3. [$(H_2O)Cl_4Os$≡N-IrClCp*(Ph_3As)]·(H_2O)

60 mg of [$(Ph_3As)_2OsNCl_3$] (0.065mmol) was dissolved in 6ml of CH_2Cl_2, 50 mg of [μ-ClIrClCp*]$_2$ (0.065mmol) dissolved in 2ml of CH_2Cl_2 was added to the pink solution. A colour change to brown was observed. A layer of n-hexane was then added, and after a few days exposed to the atmosphere, green [$(H_2O)Cl_4Os$≡N-IrClCp*(Ph_3As)]·(H_2O) crystals appeared. Yield 45%

Elemental analysis of [$(H_2O)Cl_4Os$≡N-IrClCp*(Ph_3As)]·(H_2O)

[%]	C	H	N
Experimental	37.6	2.9	1.0
Theoretical	32.0	3.2	1.3

4.3.4. [$(Ph_3Sb)_2Cl_3Os{\equiv}N$-IrCl(COD)]

40 mg of [$(Ph_3Sb)_2OsNCl_3$] (0.039mmol) was dissolved in 4ml of CH_2Cl_2, 12 mg of [μ-ClRh(COD)]$_2$ (0.020mmol) dissolved in 2ml of CH_2Cl_2 was added to the orange solution, and an immediate colour change to very dark green was observed. The solution was stirred for a further hour, and then a layer of n-hexane was carefully placed on top of the reaction solution. Dark green [$(Ph_3Sb)_2Cl_3Os{\equiv}N$-IrCl(COD)] crystals formed after a few days. Yield 80%.

Elemental analysis of [$(Ph_3Sb)_2Cl_3Os{\equiv}N$-IrCl(COD)]

[%]	C	H	N
Experimental	32.8	3.3	1.0
Theoretical	39.1	3.1	1.0

4.3.5. [$(Ph_3Sb)Cl_4Os{\equiv}N$-IrClCp*(Ph_3Sb)]

50mg of [$(Ph_3Sb)_2OsNCl_3$] (0.049mmol) was dissolved in 6ml of CH_2Cl_2, 20mg of [μ-ClIrClCp*]$_2$ (0.025mmol) was dissolved in 4ml of CH_2Cl_2, and added to the orange solution turning it brown. The solution was refluxed for 30 minutes, and then allowed to cool. The solution was transferred to a Schlenk tube and a layer of n-hexane was carefully added. Within 2 days brown, [$(Ph_3Sb)Cl_4Os{\equiv}N$-IrClCp*(Ph_3Sb)], crystals had formed. Yield 80%

Elemental analysis of [$(Ph_3Sb)Cl_4Os{\equiv}N$-IrClCp*(Ph_3Sb)]

[%]	C	H	N
Experimental	35.1	2.7	1.0
Theoretical	39.0	3.2	1.0

4.3.6. [RhCp*Cl$_2$(AsPh$_3$)]

60 mg of [(Ph$_3$As)$_2$OsNCl$_3$] (0.065mmol) was dissolved in 6ml of CH$_2$Cl$_2$, 40 mg of [μ-ClRhClCp*]$_2$ (0.065mmol) dissolved in 2ml of CH$_2$Cl$_2$ was added to the pink solution. A colour change to reddish orange was observed. A layer of n-hexane was then added, and after a few days orange [RhCp*Cl$_2$(AsPh$_3$)] crystals appeared. Yield 45%

4.4. Analysis Methods

4.4.1. Elemental Analysis

The Carbon-, Hydrogen-, and Nitrogen- content of the synthesised compounds was micro-analytically determined using incineration techniques with a CARLO ERBA Elemental Analyser, model 1104.

4.4.2. Single Crystal X-ray diffraction

The single crystal X-ray measurements were made using either an automatic ENRAF-NONIUS CAD4 diffractometer with a graphite monochromator, or a STOE IPDS diffractometer. The measurements were made using MoK$_\alpha$- or CuK$_\alpha$- radiation. The crystals were attached to the glass rods using Voltaleff vacuum grease.

The positions of the hydrogen atoms were located either using the Fourier series method, or their ideal positions were calculated using computational methods. The graphic presentations were generated using the PLATON [15], SCHAKAL [16] and DIAMOND programs. The reflection intensities were adjusted using DIFABS [15], numerical [17] or Psi-scans [15] absorption correction methods.

4.4.3. Infrared Spectroscopy

A PERKIN ELMER Spectrum 1000 FT-IR Spectrometer was used to for the IR-spectra; the spectra covered the area from 4000-200 cm^{-1}. The samples were ground together with KBr, and then pressed into tablet form of a suitable thickness for the IR Spectrometer.

4.4.4. Magnetic measurements

The magnetic measurements were made using a “Quantum Design” Squid-Magnetometer. The samples were placed in a gelatine capsule, and magnetic susceptibilities were accordingly adjusted for the diamagnetic component of the capsule. The calculations were also diamagnetically corrected according to Haberditzel [18].

4.4.5. Mass Spectrum

The mass spectra were measured using the following:
FAB^+: TSQ 70 FINNIGAN MAT.
FAB^-: MAT 711A modified by AMD-INTEKTRA.
Nitrobenzylalcohol (NBA) was used as a matrix.

4.4.6. Programs used

SHELXS97	Program for the solution of crystal structures, G.M.Sheldrick, University of Göttingen 1997 [19].
SHELXL97	Program for the calculation and refinement of crystal structures, G.M.Sheldrick, University of Göttingen 1997 [20].
HELENA, PLATON	Programs used to calculate crystal structures, A.L.Spek. University of Utrecht, Holland 1993 [21, 15].
CHECKHKL	Program to determine the space group of a crystal structure, M.Kretschmar, University of Tübingen, 1998 [22].
DIAMOND	Graphics program, Version 1.2, K.Brandenburg, 1997.
SCHAKAL	Graphics program, E. Keller, Freiburg 1992 [16].
ISIS-DRAW	Graphics program used to generate diagrams of chemical structures, Version 2.1.4, MDL Information Systems, Inc.

4.5. Archives

In addition to the tables in the appendix of this dissertation, the following tables are available on request:

- Atomic coordinates of the atoms
- Isotropic displacement parameters of the refined atoms
- Inter atomic distances and angles of all the atoms
- Observed and calculated structural factors

These tables are available from:

Prof. Dr. Dr. h.c.Joachim Strähle
Universität Tübingen
Institut für Anorganische Chemie
Auf der Morgenstelle 18
72076 Tübingen

The complete tables of the published material described in this dissertation are also deposited at the:

Cambridge Crystallographic Data Centre
12 Union Road
Cambridge
CB2 1EZ
UK

The reference numbers of the archived data are listed below.

4.5.1. Archive Reference Numbers

[(Ph$_3$As)$_2$Cl$_3$Os≡N-RhCl(COD)]	CCDC 258008
[(Ph$_3$As)$_2$Cl$_3$Os≡N-IrCl(COD)]	CCDC 258009
[(H$_2$O)Cl$_4$Os≡N-IrClCp*(Ph$_3$As)]·(H$_2$O)	CCDC xxxxxx
[(Ph$_3$Sb)$_2$Cl$_3$Os≡N-IrCl(COD)]	CCDC xxxxxx
[(Ph$_3$Sb)Cl$_4$Os≡N-IrClCp*(Ph$_3$Sb)]	CCDC xxxxxx

4.6. Publications

- D. Morrogh, M. G. Mestres, E. Niquet, C. F. Barbosa. da Silva, A. Santos Saez, S. Schwarz und J. Strähle
  Z. Anorg. Allg. Chem. **631**, 1113 (2005).
  Synthesis and Structural characterization of hetero-nuclear metal-complexes with nitrido bridges Re≡N-Ni, Re≡N-Pt, Os≡N-Rh and Os≡N-Ir

- D. Morrogh, S. Schwarz, C. Maichle-Mössmer und J. Strähle
  Synthesis, Crystal Structure and Properties of the Complexes
  Z. Anorg. Allg. Chem. In print
  $[(H_2O)Cl_4Os{\equiv}N\text{-}IrCl(C_5Me_5)(AsPh_3)]$, $[(Ph_3Sb)Cl_4Os{\equiv}N\text{-}IrCl(C_5Me_5)(SbPh_3)]$
  $[(Ph_3Sb)_2Cl_3Os{\equiv}N\text{-}IrCl(COD)]$ and
  $[\{(Me_2PhP)_2(CO)Cl_2Re{\equiv}N\}_2ReNCl_2(PMe_2Ph)]$

5. Conclusion

The aim of this study was to synthesise and structurally characterise new nitrido complexes, and investigate how nitrido ligands affect the geometry and other aspects of the synthesized complexes.

The first part of this study focussed on complexes synthesised using the starting material [$(Ph_3As)_2Cl_3OsN$], which was first synthesised by P. Griffith et al.[6], but to date no crystal structure has been published. Therefore Crystals of [$(Ph_3As)_2Cl_3OsN$] were obtained and structurally characterised using single crystal X-ray diffractometry. [$(Ph_3As)_2Cl_3OsN$] crystallises in the triclinic space group $P\bar{1}$, with a unit cell: a = 1183.69(16) pm; b = 1411.03(19) pm; c = 1634.1(2) pm; α = 115.497(15)°; β = 94.120(16)°; γ = 92.033(16)°. It consists of an octahedrally coordinated osmium atom, surrounded by a nitrido ligand, two triphenyl arsane ligands, and three chloro ligands. The two arsane groups are mutually *trans*- to one another, and *cis*- with respect to the nitrido function. The three remaining octahedral sites are occupied by the chlorine ligands.

Using the strongly basic nitrido ligand of [$(Ph_3As)_2Cl_3OsN$], it was possible to break the chloro bridges of Lewis acids of the form [μ-$ClML_x$] and thus synthesise three novel nitrido bridged complexes, the first two, [$(Ph_3As)_2Cl_3Os{\equiv}N$-$RhCl(COD)$] and [$(Ph_3As)_2Cl_3Os{\equiv}N$-$IrCl(COD)$] are isostructural, air stable, and both crystallise in the monoclinic space group Cc, with unit cells: a = 2316.8(5) pm; b = 1169.31(11) pm; c = 1601.35(17) pm; β = 106.121(11)° and a = 2322.1(2) pm; b = 1167.01(6) pm; c = 1603.77(18) pm; β = 105.927(9) ° respectively. Both have almost linear asymmetric nitrido bridges of the form Os≡N-M’, with the octahedral structure of the [$(Ph_3As)_2Cl_3OsN$] starting material preserved in the bridged compound.

The data obtained from the crystal structure of [$(Ph_3As)_2Cl_3OsN$] proved to be a very useful tool for comparing and contrasting the effects a nitrido function has on bridged complexes. The varying *trans*-Os-Cl-bond lengths are indicative of the increasing and decreasing Os-N-bond order; with the nitrido bridged complexes [$(Ph_3As)_2Cl_3Os$≡N-RhCl(COD)] and [$(Ph_3As)_2Cl_3Os$≡N-IrCl(COD)], having notably shorter *trans*-Os-Cl-bond lengths indicating, a lower Os-N-bond order than the terminal Os-N-bond order of the starting complex [$(Ph_3As)_2Cl_3OsN$].

In the nitrido bridged complexes [$(Ph_3As)_2Cl_3Os$≡N-IrCl(COD)] and [$(Ph_3As)_2Cl_3Os$≡N-RhCl(COD)], the influence of the nitrido bridge was also noted in the differing bond lengths from the rhodium and iridium atoms (M’) to the cyclo-octadiene fragment; where the M’-C-bond lengths are notably longer in *trans*-position, indicating that there is a π-component to the N-M’-bond.

The third nitrido complex synthesised using the [$(Ph_3As)_2Cl_3OsN$] starting complex was [$(H_2O)Cl_4Os$≡N-IrClCp*(Ph_3As)].(H_2O). This air stable compound crystallises in the monoclinic space group Cm with a unit cell: a = 1105.53(6) pm; b = 1486.76(9) pm; c = 2024.88(10) pm and β = 97.191(4)º. The structure of the starting material [$(Ph_3As)_2Cl_3OsN$] is not preserved in the bridged complex; the two arsane ligands vacate the osmium atom and are replaced by a chlorine atom from the dimeric iridium starting material, and a water molecule in *trans*-position to the asymmetric Os≡N-Ir nitrido bridge. The atmospheric water in *trans*-position is needed for the complex to crystallise. One of the arsane ligands from [$(Ph_3As)_2Cl_3OsN$] coordinates to the iridium atom, filling the empty octahedral site left by the migrating chlorine. The other arsane ligand probably partakes in a tandem reaction with the second half of the dimeric iridium complex to form an arsane-iridium compound, similar to the stibane-rhodium compound, [RhCp*Cl_2($AsPh_3$)] synthesized in a similar reaction.

The nitrido *trans*-influence was also noted in [$(H_2O)Cl_4Os$≡N-IrClCp*(Ph_3As)]•(H2O) where a similar lengthening of the Ir-C-bond in *trans*-

position to the nitrido bridge was observed, again indicating a π-component to the N-Ir-bond.

The nitrido complexes in the second part of this study were synthesised using the starting material $[(Ph_3Sb)_2OsNCl_3]$ as a starting complex. Crystals from this complex were obtained, and structurally analysed. Unfortunately the crystals were extremely thin, and it was only possible to determine the dimensions of the unit cell; a = 972.36 pm; b = 981.09 pm; c = 1036.98 pm; α = 11.409º; β = 109.259º; γ = 92.921º, and to confirm that the stibane ligands are arranged in *trans*- position to one another.

$[(Ph_3Sb)_2Cl_3Os{\equiv}N\text{-}IrCl(COD)]$ was synthesised in an identical fashion to the above mentioned $[(Ph_3As)_2Cl_3Os{\equiv}N\text{-}IrCl(COD)]$, with the strongly basic nitrido ligand reacting with the iridium Lewis acid to form a nitrido bridge. $[(Ph_3Sb)_2Cl_3Os{\equiv}N\text{-}IrCl(COD)]$ crystallises in the triclinic space group $P\bar{1}$, with a unit cell: a = 1079.41(14) pm; b = 1172.31(12) pm; c = 1696.72(19) pm; α = 101.192(9)º; β = 92.703(10)º; γ = 92.614(10)º. The structure of this compound is very similar to the arsane analogue described above; it consists of a close to linear Os≡N-Ir-bond, with the iridium also in a quadratic planar environment. The difference being that in this compound, the stibane ligands are *cis*- to one another, as opposed to the arsane analogue, where the arsane ligands are *trans*- to one another. This *cis*-arrangement of the stibane ligands does not reflect the geometry of the starting material $[(Ph_3Sb)_2OsNCl_3]$, meaning that a rearrangement of the chlorine and stibane ligands about the osmium atom occurs during the reaction.

The second compound, $[(Ph_3Sb)Cl_4Os{\equiv}N\text{-}IrClCp^*(Ph_3Sb)]$ crystallises in the triclinic space group $P\bar{1}$, with a unit cell: a = 1023.3(3) pm; b = 1476.2(3) pm; c = 1872.5(6) pm; α = 74.6(2)º; β = 73.84(2)º; γ = 76.191(19)º. It consists of an Os≡N-Ir unit, and differs from the above described compound in that a two way migration occurs, with chlorine leaving the iridium for the osmium atom, and a stibane ligand migrating from the osmium to the iridium atom. $[(Ph_3Sb)Cl_4Os{\equiv}N\text{-}IrClCp^*(Ph_3Sb)]$ crystals from this reaction only formed when the reaction mixture was heated, an indication that perhaps an energy input is required for the migration to take place.

The last compound, [RhCp*Cl_2($AsPh_3$)], is a by-product of a failed attempt to synthesize the rhodium analogue to the [(H_2O)Cl_4Os≡N-IrClCp*(Ph_3As)]•(H_2O) complex. In both cases a tandem reaction obviously occurs, with one of the arsane ligands leaving the osmium atom to fill a vacant site on the iridium/rhodium, and the other arsane ligand reacting with the second half of the iridium/rhodium dimer to form a compound of the form [M'Cp*Cl_2($AsPh_3$)]. In this case [RhCp*Cl_2($AsPh_3$)] crystallizes in the monoclinic space group Cm with a unit cell: a = 8608.6(4) pm; b = 32276.4(18) pm; c = 18257.9(9) pm; β = 90.372(4)º.

6. Appendix

6.1. Abbreviations Legend

The following initials and abbreviations were used in this thesis;

μ_{exp}	experimental magnetic moment
χ_{mol}	molar susceptibility
$\chi_{mol, corr}$	molar susceptibility, corrected
COD	Cylcoocta-1, 5-diene
Cp*	Pentamethylcyclopentadienyl
emu	electromagnetic unit
FAB	Fast Atom Bombardment
Me	Methyl
Ph	Phenyl
NMP	N-Methyl-Pyrolidone
SQUID	Superconducting Quantum Interference Device
st	strong
w	weak

6.2. Definitions

6.2.1. R-Values

The agreement between the measured and calculated crystal structures is quantified by R-values. These equations are a sum of the discrepancies between the calculated and observed structures for the reflections measured.

$$\mathrm{R}_1 = \frac{\sum_{hkl} \left\| F_0(hkl) \right| - \left| F_c(hkl) \right\|}{\sum_{hkl} \left| F_0(hkl) \right|}$$

For the wR$_2$ calculation, the SHELXL97 program uses the following weighting scheme:

$$\omega(hkl) = \frac{1}{\left[\sigma^2 F_o^2(hkl) + (aP)^2 + bP\right]}$$

$$\text{with: } P = \frac{1}{3}\max\left(0, F_0^2\right) + \frac{2}{3}F_c^2$$

The parameters *a* and *b* are so adjusted that if possible there is an equal distribution of the variation of the different diffraction angles and intensity areas.

$$\omega R_2 = \sqrt{\frac{\sum_{hkl} \omega(hkl)\left(F_o^2(hkl) - F_c^2(hkl)\right)^2}{\sum_{hkl} \omega(hkl)\left(F_o^2(hkl)\right)^2}}$$

The “Goodness of fit” parameter describes the degree of agreement between the structure solution and the actual structure.

$$GooF = \sqrt{\frac{\sum_{hkl} \omega(hkl)\left(F_o^2(hkl) - F_c^2(hkl)\right)^2}{n - p}}$$

where n = number of reflections, p = number of parameters

The difference n-p defines the agreement of the structural parameters. When the correct weighting is used, the GooF value should be under 1.

6.2.2. Displacement parameter

The Displacement parameter U_{eq} is defined as a third of the peak of the orthogonal U_{ij}-Tensors [23].

$$U_{eq} = \frac{1}{3} \sum_i \sum_j U_{ij} a_i^* a_j^* a_i a_j$$

6.3. Atomic Coordinates and Isotropic Displacement Parameters

6.3.1. [$(Ph_3As)_2Cl_3Os{\equiv}N$]

Table 6.3.1. Atomic coordinates and equivalent isotropic displacement parameters U_{eq} [$10pm^2$] for [$(Ph_3As)_2Cl_3Os{\equiv}N$]

Atom	x	y	z	U_{eq}
Os(1)	0.0000	0.0000	0.5000	46(1)
N(1)	-0.0084(14)	-0.1454(15)	0.4652(11)	38(1)
Cl(11)	0.0173(2)	0.0238(1)	0.6522(1)	39(1)
Cl(12)	-0.0206(3)	-0.1755(3)	0.4533(3)	38(1)
As(11)	-0.2154(1)	-0.0069(1)	0.4905(1)	27(1)
C(111)	-0.2748(5)	0.1289(5)	0.5206(4)	32(1)
C(112)	-0.3513(6)	0.1692(5)	0.5859(5)	37(2)
C(113)	-0.3889(7)	0.2683(5)	0.6080(5)	47(2)
C(114)	-0.3535(7)	0.3252(5)	0.5630(6)	50(2)
C(115)	-0.2804(6)	0.2854(5)	0.4972(6)	46(2)
C(116)	-0.2397(6)	0.1868(5)	0.4763(5)	40(2)
C(121)	-0.2821(5)	-0.0556(4)	0.5710(4)	30(1)
C(122)	-0.3544(6)	-0.1464(5)	0.5347(5)	37(2)
C(123)	-0.4059(7)	-0.1785(6)	0.5929(6)	50(2)
C(124)	-0.3867(7)	-0.1231(6)	0.6842(5)	45(2)
C(125)	-0.3127(6)	-0.0329(6)	0.7214(5)	42(2)
C(126)	-0.2614(6)	0.0006(5)	0.6641(5)	38(2)
C(131)	-0.2934(5)	-0.0950(4)	0.3724(4)	29(1)
C(132)	-0.3926(6)	-0.0656(6)	0.3450(5)	43(2)
C(133)	-0.4537(6)	-0.1316(6)	0.2616(5)	49(2)
C(134)	-0.4139(7)	-0.2260(6)	0.2073(5)	51(2)
C(135)	-0.3129(7)	-0.2550(6)	0.2337(6)	56(2)
C(136)	-0.2516(7)	-0.1904(5)	0.3171(5)	47(2)
Os(2)	0.3442(1)	0.3244(1)	0.1715(1)	27(1)

N(2)	0.3502(4)	0.3498(4)	0.2884(5)	45(2)
C1(21)	0.3851(2)	0.5026(l)	0.2053(l)	39(l)
C1(22)	0.3376(2)	0.2962(1)	0.0116(1)	37(1)
Cl(23)	0.2987(2)	0.1418(1)	0.1105(1)	38(1)
As(21)	0.5590(1)	0.3134(1)	0.1695(1)	27(1)
C(211)	0.6244(5)	0.1901(5)	0.1717(4)	31(l)
C(212)	0.7227(6)	0.2021(5)	0.2273(5)	38(2)
C(213)	0.7712(7)	0.1126(6)	0.2288(5)	44(2)
C(214)	0.7197(7)	0.0136(5)	0.1724(5)	45(2)
C(215)	0.6231(7)	0.0023(5)	0.1172(5)	44(2)
C(216)	0.5745(6)	0.0902(5)	0.1158(5)	38(2)
C(221)	0.6354(6)	0.4272(4)	0.2783(5)	41(2)
C(222)	0.6000(7)	0.4409(6)	0.3613(5)	52(2)
C(223)	0.6517(9)	0.5232(7)	0.4398(6)	73(3)
C(224)	0.7359(9)	0.5898(7)	0.4356(9)	84(4)
C(225)	0.7722(8)	0.5738(6)	0.3541(9)	77(4)
C(226)	0.7210(7)	0.4927(6)	0.2729(7)	57(2)
C(231)	0.0627(5)	0.3302(5)	0.0705(4)	31(l)
C(232)	0.6060(6)	0.4216(5)	0.0589(5)	39(2)
C(233)	0.6510(6)	0.4339(5)	-0.0110(5)	45(2)
C(234)	0.7129(7)	0.3579(6)	-0.0696(6)	49(2)
C(235)	0.7292(7)	0.2672(6)	-0.0591(6)	50(2)
C(236)	0.6830(6)	0.2530(5)	0.0118(5)	42(2)
As(22)	0.1306(1)	0.3385(1)	0.1614(1)	27(1)
C(241)	0.0423(5)	0.2265(4)	0.0601(4)	30(1)
C(242)	0.0631(6)	0.2029(5)	-0.0281(5)	40(2)
C(243)	0.0024(7)	0.1190(6)	-0.1006(5)	50(2)
C(244)	-0.0785(6)	0.0587(5)	-0.0832(5)	46(2)
C(245)	-0.1017(6)	0.0820(5)	0.0034(5)	45(2)
C(246)	-0.0400(6)	0.1658(5)	0.0768(5)	35(1)
C(251)	0.0755(5)	0.3294(4)	0.2664(4)	30(1)
C(252)	0.1104(5)	0.2507(5)	0.2898(4)	32(1)
C(253)	0.0711(6)	0.2425(5)	0.3636(5)	38(2)

C (254)	-0.0032 (6)	0.3126(5)	0.4157 (5)	42(2)
C(255)	-0.0383(6)	0.3904(6)	0.3924(5)	44(2)
C(256)	-0.0007(6)	0.3978(5)	0.3172(5)	36(1)
C(261)	0.0746(6)	0.4680(4)	0.1670(4)	32(1)
C(262)	0.1183(6)	0.5620(5)	0.2387(5)	38(2)
C(263)	0.0744(6)	0.6563(5)	0.2483(6)	45(2)
C(264)	-0.0119(7)	0.6550(6)	0.1869(6)	53(2)
C(265)	-0.0547(8)	0.5622(6)	0.1155(6)	53(2)
C(266)	-0.0116(6)	0.4677(5)	0.1069(5)	42(2)

6.3.2 $[(Ph_3As)_2Cl_3Os\equiv N\text{-}RhCl(COD)]$

Table 6.3.2. Atomic coordinates and equivalent isotropic displacement parameters U_{eq} [10pm^2] for $[(Ph_3As)_2Cl_3Os\equiv N\text{-}RhCl(COD)]$

Atom	x	y	z	U_{eq}
Os	0.0002(l)	0.2746(l)	0.2519(l)	31(l)
Rh	-0.0065(1)	0.5757(1)	0.2598(1)	41(1)
As(1)	0.1013(l)	0.2518(2)	0.3629(l)	35(l)
As(2)	-0.1023(1)	0.2626(2)	0.1406(1)	35(1)
Cl(1)	-0.0399(2)	0.2516(5)	0.3721(3)	44(1)
Cl(2)	0.401(3)	0.2724(5)	0.1301(4)	49(1)
Cl(3)	0.0032(3)	0.0685(3)	0.2443(4)	51(1)
Cl(4)	-0.0912(2)	0.5534(4)	0.3118(4)	63(1)
N	-0.0015(6)	0.4178(8)	0.2531(10)	25(2)
C(1)	-0.0035(10)	0.7629(15)	0.2997(14)	53(5)
C(2)	-0.0331(8)	0.7587(15)	0.2117(16)	58(6)
C(3)	-0.0035(11)	0.7875(19)	0.1431(14)	69(6)
C(4)	0.0257(9)	0.6909(17)	0.1089(11)	60(5)
C(5)	0.0483(8)	0.5965(13)	0.1759(12)	45(4)
C(6)	0.0837(8)	0.6156(15)	0.2616(12)	53(4)
C(7)	0.1047(10)	0.7321(16)	0.2964(13)	65(6)
C(8)	0.0601(11)	0.7927(17)	0.3401(14)	70(6)
C(11)	0.1066(10)	0.1541(19)	0.4633(16)	49(6)
C(13)	0.1602(8)	0.1036(17)	0.6115(13)	50(5)
C(12)	0.1534(8)	0.1790(2)	0.5377(15)	53(5)
C(14)	0.1217(10)	0.0180(2)	0.6110(15)	52(5)
C(15)	0.0751(12)	0.0030(2)	0.0368(14)	62(6)
C(16)	0.0672(10)	0.0648(16)	0.4639 (14)	50(5)
C(21)	0.1312(8)	0.3937 (19)	0.0410 (11)	38(4)
C(22)	0.0933(13)	0.4580(2)	0.4521(16)	58(6)
C(23)	0.1118(14)	0.5600(2)	0.4913(15)	70(8)
C(24)	0.1703 (12)	0.6020(3)	0.4988 (15)	73(7)

C(25)	0.2082 (13)	0.5400(2)	0.4662 (18)	69(7)
C(26)	0.1887(10)	0.4346(18)	0.4234(14)	49(5)
C(31)	0.1654(10)	0.1970(2)	0.3166(15)	49(5)
C(32)	0.1796(10)	0.2604(17)	0.2522(18)	50(6)
C(33)	0.2288 (10)	0.2200(3)	0.2235 (17)	63(8)
C(34)	0.2595(10)	0.1230(2)	0.2564(16)	60(6)
C(35)	0.2445 (10)	0.0670(2)	0.3207 (17)	63(7)
C(36)	0.1968(12)	0.0990(2)	0.3494(16)	59(6)
C(41)	-0.1319(9)	0.4099(16)	0.0904(13)	39(4)
C(42)	-0.0984(8)	0.4711(18)	0.0499(15)	46(5)
C(43)	-0.1207(10)	0.5747(18)	0.0092(16)	53(6)
C(44)	-0.1735(14)	0.6140(2)	0.0140(16)	69(7)
C(45)	-0.2095(11)	0.5545(19)	0.0555(16)	54(6)
C(46)	-0.1882(11)	0.4490(2)	0.0898(15)	57(6)
C(51)	-0.1652(7.)	0.2079 (17)	0.1852 (12)	34(4)
C(52)	-0.1798(8)	0.2620(2)	0.2533(13)	47(6)
C(53)	-0.2233(10)	0.2266(19)	0.2885(16)	51(6)
C(54)	-0.2562(11)	0.1320(3)	0.2553(17)	69(8)
C(55)	-0.2444(11)	0.0730(2)	0.1867(17)	68(8)
C(56)	-0.1991(9)	0.1130(2)	0.1511(15)	51(5)
C(61)	-0.1092(7)	0.1718 (16)	0.0382(13)	34(4)
C(62)	-0.1379(14)	0.2110(2)	-0.0423(16)	89(10)
C(63)	-0.1434(13)	0.1440(2)	-0.1159(15)	83(9)
C(64)	-0.1223(9)	0.0370(2)	-0.1099(15)	56(6)
C(65)	-0.0947(16)	-0.0010(3)	-0.0323(17)	113(14)
C(66)	-0.0910(16)	0.0660(2)	0.0415(15)	106(13)

6.3.3 [(Ph$_3$As)$_2$Cl$_3$Os≡N-IrCl(COD)]

Table 6.3.3. Atomic coordinates and equivalent isotropic displacement parameters U_{eq} [10pm^2] for [(Ph$_3$As)$_2$Cl$_3$Os≡N-IrCl(COD)]

Atom	x	y	z	U_{eq}
Ir	-0.0055(1)	0.0759(1)	0.7541(1)	44(l)
Os	0.0008(1)	-0.2257(1)	0.7476(1)	26(l)
As(1)	0.1017(1)	-0.2455(2)	0.8577(1)	31(l)
As(2)	-0.1010(1)	-0.2391(2)	0.6368(1)	31(l)
Cl(1)	-0.0398(2)	-0.2433(4)	0.8682(3)	44(l)
Cl(2)	0.0407(2)	-0.2308(4)	0.6262(3)	43(1)
Cl(3)	0.0011(4)	-0.4325(2)	0.7438(5)	55(l)
Cl(4)	-0.0921(2)	0.0582(4)	0.8063(3)	64(l)
N	-0.0004(7)	-0.0790(7)	0.7490(11)	24(2)
C(1)	-0.0211(16)	0.2617(16)	0.7057(12)	133(15)
C(2)	-0.0138(16)	0.267(2)	0.772(5)	220(3)
C(3)	0.0594(9)	0.2904(16)	0.8327(13)	71(5)
C(4)	0.1034(8)	0.2355(14)	0.7911(10)	62(5)
C(5)	0.0819(7)	0.1146(15)	0.7572(10)	58(4)
C(6)	0.0442(7)	0.0978(12)	0.6695(9)	45(3)
C(7)	0.0255(7)	0.1922(15)	0.6060(10)	60(4)
C(8)	-0.0037(12)	0.2911(15)	0.6389(13)	90(8)
C(11)	0.1081(8)	-0.3441(17)	0.9608(12)	38(4)
C(12)	0.0711(10)	-0.4332(16)	0.9605(14)	55(5)
C(13)	0.0785(10)	-0.499(2)	1.0319(12)	59(5)
C(14)	0.1224(9)	-0.480(2)	1.1043(13)	56(5)
C(15)	0.1604(9)	-0.379(2)	1.1097(14)	69(6)
C(16)	0.1532(8)	-0.3188(18)	1.0335(13)	52(4)
C(21)	0.1313(7)	-0.1023(15)	0.9124(10)	34(4)
C(22)	0.0965(9)	-0.0417(17)	0.9486(12)	44(4)
C(23)	0.1161(13)	0.0690(19)	0.9908(14)	68(7)
C(24)	0.1732(11)	0.103(2)	0.9929(13)	62(6)

C(25)	0.2091(11)	0.040(2)	0.9586(17)	69(6)
C(26)	0.1902(9)	-0.0623(15)	0.9182(14)	46(4)
C(31)	0.1662(8)	-0.3023(17)	0.8134(10)	40(4)
C(32)	0.1798(8)	-0.2371(16)	0.7467(14)	49(5)
C(33)	0.2281(8)	-0.278(2)	0.7188(15)	59(6)
C(34)	0.2559(8)	-0.373(2)	0.7468(12)	64(7)
C(35)	0.2443(11)	-0.435(2)	0.8153(17)	69(7)
C(36)	0.1957(10)	-0.3988(17)	0.8455(13)	55(6)
C(41)	-0.1639(7)	-0.2960(15)	0.6834(10)	33 (3)
C(42)	-0.1969(8)	-0.3926(19)	0.6482(12)	50(5)
C(43)	-0.2422(10)	-0.434(2)	0.6811(13)	63(7)
C(44)	-0.2584(9)	-0.375(2)	0.7450(14)	63(6)
C(45)	-0.2230(8)	-0.2789(18)	0.7830(12)	48(5)
C(46)	-0.1794(7)	-0.2424(16)	0.7500(10)	40(4)
C(51)	-0.1076(7)	-0.3299(15)	0.5344(10)	31(4)
C(52)	-0.0779(15)	-0.431(2)	0.5367(13)	116(13)
C(53)	-0.0882(15)	-0.503(2)	0.4609(15)	109(11)
C(54)	-0.1221(8)	-0.4633(17)	0.3849(12)	47(4)
C(55)	-0.1480(13)	-0.373(3)	0.3866(17)	108(12)
C(56)	-0.1411(12)	-0.294(2)	0.4546(16)	89(8)
C(61)	-0.1326(8)	-0.0930(14)	0.5865(11)	36(4)
C(62)	-0.1865(9)	-0.0512(17)	0.5860(13)	49(5)
C(63)	-0.2074(11)	0.0523(17)	0.5495(15)	58(6)
C(64)	-0.1716(10)	0.1143(18)	0.5064(14)	59(5)
C(65)	-0.1185(10)	0.0716(18)	0.5068(15)	56(6)
C(66)	-0.0963(8)	-0.0260(19)	0.5439(13)	44(5)

6.3.4. $[(H_2O)Cl_4Os{\equiv}N\text{-}IrClCp^*(Ph_3As)].(H_2O)$

Table 6.3.4. Atomic coordinates and equivalent isotropic displacement parameters U_{eq} [10pm^2] for $[(H_2O)Cl_4Os{\equiv}N\text{-}IrClCp^*(Ph_3As)].(H_2O)$

Atom	x	y	z	U_{eq}
Ir	0.8420(1)	8156(1)	0.2413(1)	17(1)
Os	1.0075(1)	0.8865(1)	0.1092(1)	17(1)
As	0.6352(1)	0.8522(1)	0.1888(1)	18(1)
Cl(1)	0.8416(3)	0.8872(2)	0.0235(2)	26(1)
Cl(2)	1.0007(3)	1.0443(2)	0.1201(l)	23(l)
Cl(3)	1.1969(3)	0.8961(3)	0.1749(2)	28(1)
Cl(4)	1.0477(4)	0.7407(2)	0.0754(2)	33(l)
Cl (5)	0.8427(3)	0.9635(2)	0.2878(2)	28(l)
N	0.9232(9)	0.8573(8)	0.1691(5)	19(2)
O(1)	1.1168(8)	0.9190(7)	0.0276(4)	26(2)
O(2)	0.8712(10)	0.4999(8)	0.0051(5)	142(4)
C(10)	0.9839(13)	0.7153(11)	0.2748(6)	27(3)
C(18)	1.1110(14)	0.7018(10)	0.2533(7)	28(3)
C(20)	0.8763(12)	0.6698(9)	0.2459(5)	18(3)
C(28)	0.8706(15)	0.5983(11)	0.1941(7)	35(4)
C(30)	0.7831(15)	0.6890(9)	0.2882(7)	31(3)
C(38)	0.6634(16)	0.6361(14)	0.2836(11)	50(5)
C(40)	0.8320(14)	0.7480(10)	0.3385(6)	29(3)
C(48)	0.7676(16)	0.7880(12)	0.3945(7)	38(4)
C(50)	0.9598(13)	0.7656(11)	0.3308(7)	30(3)
C(58)	1.0442(16)	0.8189(12)	0.3761(8)	40(4)
C(11)	0.6051(13)	0.9605(10)	0.1378(6)	25(3)
C(12)	0.6958(14)	1.0222(10)	0.1301(7)	30(3)
C(13)	0.5522(15)	1.1142(10)	0.0616(7)	31(3)
C(14)	0.6679(15)	1.0973(10)	0.0902(8)	33(3)
C(15)	0.4640(16)	1.0530(12)	0.0699(8)	40(4)
C(16)	0.4872(12)	0.9766(12)	0.1078(6)	32(4)

C(21)	0.5250(12)	0.8694(10)	0.2578(7)	25(3)
C(22)	0.5295(15)	0.9574(13)	0.2847(7)	39(4)
C(23)	0.4594(17)	0.9747(16)	0.3365(8)	51(5)
C(24)	0.3867(18)	0.9054(17)	0.3577(7)	55(6)
C(25)	0.3854(17)	0.8228(15)	0.3302(8)	51(5)
C(26)	0.4565(14)	0.8040(11)	0.2799(7)	32(3)
C(31)	0.5621(12)	0.7606(10)	0.1275(6)	23(3)
C(32)	0.4380(15)	0.7456(12)	0.1174(7)	36(4)
C(33)	0.3882(17)	0.6843(12)	0.0701(8)	44(4)
C(34)	0.4688(19)	0.6399 (13)	0.0333(8)	47(5)
C(35)	0.5909(19)	0.6563(12)	0.0411(7)	44(5)
C(36)	0.6404(14)	0.7198 (10)	0.0882(6)	27(3)

6.3.5. $[(Ph_3Sb)_2Cl_3Os{\equiv}N\text{-}IrCl(COD)]$

Table 6.3.5. Atomic coordinates and equivalent isotropic displacement parameters U_{eq} [10pm^2] for $[(Ph_3Sb)_2Cl_3Os{\equiv}N\text{-}IrCl(COD)]$

Atom	x	Y	Z	U_{eq}
Os	0.2515(1)	0.2413(1)	0.3030(1)	17(1)
Ir	0.5781(1)	0.2912(1)	0.3244(1)	22(1)
N	0.4095(10)	0.2713(10)	0.3148(6)	21(2)
Cl(1)	0.2299(3)	0.2009(3)	0.4359(2)	29(1)
Cl(2)	0.1768(3)	0.4282(3)	0.3548(2)	33(1)
Cl(3)	0.0364(3)	0.1680(3)	0.2608(2)	29(1)
Cl(4)	0.6020(4)	0.2011(3)	0.1915(2)	38(1)
Sb(1)	0.2726(4)	0.0141(1)	0.2669(l)	19(1)
Sb(2)	0.2527(1)	0.3192(1)	0.1679(1)	18(1)
C(1)	0.7859(1)	0.3419(17)	0.3403(11)	45(4)
C(2)	0.7668(14)	0.2364(16)	0.3626(10)	40(4)
C(3)	0.7599(18)	0.2189(16)	0.4461(10)	49(4)
C(4)	0.6836(15)	0.3061(14)	0.4990(9)	38(3)
C(5)	0.5746(15)	0.3405(13)	0.4549(7)	33(3)
C(6)	0.5743(14)	0.4433(13)	0.4166(8)	35(3)
C(7)	0.6897(17)	0.5194(14)	0.4140(11)	50(5)
C(8)	0.8081(16)	0.4589(15)	0.3959(12)	50(5)
C(11)	0.1406(12)	-0.0907(11)	0.3169(7)	24(3)
C(12)	0.1489(15)	-0.2109(12)	0.2921(9)	34(3)
C(13)	0.0724(16)	-0.2862(14)	0.3230(11)	44(4)
C(14)	-0.0086(13)	-0.2410(15)	0.3826(9)	38(4)
C(15)	-0.0173(12)	-0.1252(14)	0.4065(9)	36(3)
C(16)	0.0587(13)	-0.0494(12)	0.3711(9)	31(3)
C(21)	0.4372(11)	-0.0432(11)	0.3157(8)	22(2)
C(22)	0.4330(12)	-0.0782(13)	0.3897(8)	29(3)
C(23)	0.5405(14)	-0.1148(14)	0.4244(8)	35(3)
C(24)	0.6510(14)	-0.1188(14)	0.3854(9)	34(3)

C(25)	0.6557(13)	-0.0845(13)	0.3125(8)	30(3)
C(26)	0.5514(13)	-0.0455(12)	0.2778(8)	30(3)
C(31)	0.2625(12)	-0.0773(11)	0.1457(6)	24(3)
C(32)	0.3382(14)	-0.1678(13)	0.1205(9)	35(3)
C(33)	0.3226(15)	-0.2311(14)	0.0414(10)	42(4)
C(34)	0.2335(16)	-0.2050(15)	-0.0110(9)	42(4)
C(35)	0.1545(17)	-0.1123(15)	0.0146(9)	43(4)
C(36)	0.1688(14)	-0.0516(12)	0.0932(8)	30(3)
C(41)	0.2586(11)	0.2127(11)	0.0519(6)	19(2)
C(42)	0.3614(11)	0.1476(13)	0.0290(8)	28(3)
C(43)	0.3604(14)	0.0776(12)	-0.0471(8)	30(3)
C(44)	0.2609(14)	0.0730(13)	-0.1009(7)	30(3)
C(45)	0.1619(15)	0.1389(12)	-0.0797(9)	33(3)
C(46)	0.1604(13)	0.2119(12)	-0.0034(8)	26(3)
C(51)	0.1060(12)	0.4257(11)	0.1481(7)	24(3)
C(52)	-0.0146(13)	0.4037(14)	0.1684(9)	33(3)
C(53)	-0.1078(13)	0.4765(14)	0.1573(10)	37(4)
C(54)	-0.0794(14)	0.5708(15)	0.1202 (11)	42(4)
C(55)	0.1303(13)	0.5222(13)	0.1125(9)	32(3)
C(56)	0.0390(15)	0.5934(14)	0.0984(11)	41(4)
C(61)	0.3996(11)	0.4459(11)	0.1712(8)	21(2)
C(62)	0.4792(13)	0.4455(12)	0.1072(8)	28(3)
C(63)	0.5660(13)	0.5334(14)	0.1099(10)	38(4)
C(64)	0.5837(13)	0.6244(13)	0.1744(10)	37(4)
C(65)	0.5076(14)	0.6260(14)	0.2395(10)	38(3)
C(66)	0.4160(13)	0.5358(12)	0.2369(8)	29(3)

6.3.6. [$(Ph_3Sb)Cl_4Os{\equiv}N$-$IrClCp^*(Ph_3Sb)$]

Table 6.3.6. Atomic coordinates and equivalent isotropic displacement parameters U_{eq} [$10pm^2$] for [$(Ph_3Sb)Cl_4Os{\equiv}N$-$IrClCp^*(Ph_3Sb)$]

Atom	x	y	z	U_{eq}
Ir	0.5262(2)	0.7361(1)	0.3323(1)	35(1)
Os	0.2410(2)	0.7631(1)	0.2463(1)	39(1)
N	0.3780(4)	0.7420(3)	0.2900(3)	48(10)
Sb(1)	0.3510(4)	0.6752(3)	0.1334(2)	50(l)
Sb(2)	0.3566(3)	0.7806(2)	0.4554(2)	39(1)
Cl (1)	0.1718(13)	0.6140(9)	0.3084(7)	47(3)
Cl(2)	0.0878(14)	0.8355(10)	0.3431(8)	55(3)
Cl(3)	0.2874(16)	0.9161(11)	0.1766(9)	65(4)
Cl(4)	0.0436(16)	0.8005(12)	0.1876(9)	68(4)
Cl(5)	0.5061(13)	0.5774(9)	0.4023(7)	47(3)
C(11)	0.5270(6)	0.5630(4)	0.1420(3)	57(14)
C(12)	0.5370(5)	0.5270(4)	0.2170(3)	49(13)
C(13)	0.6330(8)	0.4390(6)	0.2360(5)	90(2)
C(14)	0.7360(7)	0.4110(5)	0.1710(4)	79(19)
C(15)	0.7160(8)	0.4510(6)	0.1060(5)	100(2)
C(16)	0.6170(7)	0.5320(5)	0.0960(4)	70(17)
C(21)	0.2240(8)	0.5920(6)	0.1200(5)	80(2)
C(22)	0.2510(7)	0.5000(5)	0.1470(4)	73(18)
C(23)	0.1760(10)	0.4280(7)	0.1370(6)	120(3)
C(24)	0.0620(7)	0.4670(5)	0.1050(4)	75(18)
C(25)	0.0280(10)	0.5720(7)	0.0750(6)	120(3)
C(26)	0.1160(7)	0.6240(5)	0.0860(4)	75(18)
C(31)	0.4270(7)	0.7390(5)	0.0190(4)	71(17)
C(32)	0.4190(8)	0.7080(5)	-0.0440(5)	80(2)
C(33)	0.4680(10)	0.7430(7)	-0.1150(6)	110(3)
C(34)	0.5380(11)	0.8170(8)	-0.1380(6)	120(3)
C(35)	0.5440(9)	0.8700(6)	-0.0730(5)	100(3)

C(36)	0.4880(6)	0.8280(4)	0.0010(3)	53(13)
C(41)	0.2070(4)	0.7020(3)	0.5240(2)	29(9)
C(42)	0.1360(5)	0.6530(4)	0.5010(3)	47(12)
C(43)	0.0330(6)	0.6020(4)	0.5530(3)	52(13)
C(44)	0.0010(5)	0.6070(4)	0.6240(3)	47(12)
C(45)	0.0640(6)	0.6550(4)	0.6580(3)	56(14)
C(46)	0.1690(6)	0.7090(4)	0.6020(4)	62(15)
C(51)	0.4670(6)	0.7560(4)	0.5410(3)	54(14)
C(52)	0.5390(6)	0.6670(4)	0.5600(3)	58(14)
C(53)	0.6160(6)	0.6460(4)	0.6190(3)	52(13)
C(54)	0.6210(8)	0.7230(6)	0.6470(5)	90(2)
C(55)	0.5520(8)	0.8120(5)	0.6280(4)	80(2)
C(56)	0.4810(5)	0.8350(4)	0.5680(3)	49(13)
C(61)	0.2600(4)	0.9230(3)	0.4490(2)	26(9)
C(62)	0.1900(5)	0.9630(3)	0.5150(3)	38(11)
C(63)	0.1220(7)	1.0530(5)	0.5120(4)	71(17)
C(64)	0.1310(7)	1.1200(5)	0.4310(4)	73(18)
C(65)	0.1750(8)	1.0840(6)	0.3730(5)	90(2)
C(66)	0.2610(6)	0.9810(4)	0.3720(3)	57(14)
C(10)	0.6790(5)	0.7610(4)	0.2310(3)	44(12)
C(18)	0.6760(6)	0.7730(4)	0.1470(4)	62(15)
C(20)	0.7490(6)	0.7030(5)	0.2760(4)	65(16)
C(28)	0.8230(6)	0.5980(4)	0.2610(3)	61(15)
C(30)	0.7430(3)	0.7220(2)	0.3420(18)	12(7)
C(38)	0.7970(7)	0.6580(5)	0.4210(4)	71(17)
C(40)	0.6830(5)	0.8230(4)	0.3370(3)	48(12)
C(48)	0.6850(7)	0.8920(5)	0.3810(4)	72(18)
C(50)	0.6420(5)	0.8460(3)	0.2630(3)	35(10)
C(58)	0.5960(6)	0.9590(4)	0.2250(3)	54(14)

6.3.7. [(Ph$_3$As)RhCl$_2$Cp*]

Table 6.3.7. Atomic coordinates and equivalent isotropic displacement parameters U_{eq} [10pm^2] for [(Ph$_3$As)RhCl$_2$Cp*]

Atom	x	y	z	U_{eq}
Rh(1)	0.8975(1)	0.9650(1)	0.6789(1)	15(1)
Rh(2)	0.4118(1)	0.7981(1)	0.4781(1)	15(1)
As(1)	0.9392(1)	0.9841(1)	0.8074(1)	17(1)
As(2)	0.5283(1)	0.7720(1)	0.3651(1)	17(1)
Cl(11)	1.1606(2)	0.9396(1)	0.6815(1)	31(1)
Cl(12)	0.9834(2)	1.0335(1)	0.6477(1)	26(1)
Cl(21)	0.4093(2)	0.7276(1)	0.5192(1)	26(1)
Cl(22)	0.6728(2)	0.8094(1)	0.5235(1)	24(1)
C(1)	0.7506(7)	0.9615(2)	0.5799(3)	21(1)
C(18)	0.7525(8)	0.9903(2)	0.5160(3)	28(1)
C(2)	0.8339(7)	0.9243(2)	0.5873(3)	20(1)
C(28)	0.9438(7)	0.9054(2)	0.5331(3)	26(1)
C(3)	0.7931(7)	0.9056(2)	0.6571(3)	21(1)
C(38)	0.8501(8)	0.8646(2)	0.6829(4)	30(1)
C(4)	0.6796(7)	0.9316(2)	0.6906(3)	24(1)
C(48)	0.5877(7)	0.9224(2)	0.7583(4)	31(2)
C(5)	0.6573 (6)	0.9674(2)	0.6447(3)	21(l)
C(58)	0.5387(7)	1.0007(2)	0.6560(4)	31(2)
C(6)	0.1704(7)	0.8140(2)	0.4553(3)	21(1)
C(68)	0.0507(7)	0.7930(2)	0.4100(4)	38(2)
C(7)	0.2686(7)	0.8477(2)	0.4331(3)	21(1)
C(78)	0.2691(8)	0.8668(2)	0.3588(4)	35(2)
C(8)	0.3498(7)	0.8622(2)	0.4964(4)	26(1)
C(88)	0.4555(9)	0.8989(2)	0.5011(4)	40(2)
C(9)	0.3017(7)	0.8378(2)	0.5580(3)	26(1)
C(98)	0.3590(10)	0.8435(3)	0.6356(4)	49(2)
C(10)	0.1896(7)	0.8092(2)	0.5332(4)	26(1)

C(108)	0.1002(8)	0.7791(2)	0.5789(4)	43(2)
C(11)	0.8545(7)	1.0361(2)	0.8434(3)	20(1)
C(12)	0.7637(7)	1.0608(2)	0.7980(3)	24(1)
C(13)	0.7115(8)	1.0988(2)	0.8230(4)	31(2)
C(14)	0.7506(9)	1.1127(2)	0.8922(4)	35(2)
C(15)	0.8431(9)	1.0887(2)	0.9365(4)	35(2)
C(16)	0.8948(8)	1.0504(2)	0.9128(3)	27(1)
C(21)	1.1533(7)	0.9938(2)	0.8372(3)	20(l)
C(22)	1.2265(7)	1.0283(2)	0.8079(3)	26(l)
C(23)	1.3717(7)	1.0395(2)	0.8317(4)	32(2)
C(24)	1.4491(7)	1.0159(2)	0.8840(4)	32(2)
C(25)	1.3770(8)	0.9810(2)	0.9123(4)	34(2)
C(26)	1.2295(7)	0.9700(2)	0.8892(4)	29(1)
C(31)	0.8746(7)	0.9428(2)	0.8784(3)	19(1)
.C(32)	0.7797(7)	0.9503(2)	0.9374(3)	26(1)
C(33)	0.7368(8)	0.9180(2)	0.9835(4)	34(2)
C (34)	0.7900(8)	0.8785(2)	0.9715(4)	33(2)
C(35)	0.8884(8)	0.8705(2)	0.9134 (3)	27(l)
C(36)	0.9280(7)	0.9024(2)	0.8663(3)	25(l)
C(41)	0.6545(6)	0.7218(2)	0.3710(3)	18(1)
C(42)	0.6531(7)	0.6922(2)	0.3162(3)	25(l)
C(43)	0.7469(8)	0.6571(2)	0.3212(4)	29(2)
C(44)	0.8437(8)	0.6522(2)	0.3807(4)	33(2)
C(45)	0.8487(8)	0.6816(2)	0.4353(4)	33(2)
C(46)	0.7544(7)	0.7165(2)	0.4317(3)	24(l)
C(51)	0.3729(7)	0.7578(2)	0.2913(3)	20(1)
C(52)	0.3625(8)	0.7776(2)	0.2240(3)	28(1)
C(53)	0.2414(8)	0.7688(2)	0.1771(4)	33(2)
C(54)	0.1295(7)	0.7399(2)	0.1961(4)	29(1)
C(55)	0.1390(7)	0.7198(2)	0.2626(4)	27(1)
C(56)	0.2603(7)	0.7289(2)	0.3109(3)	26(1)
C(61)	0.6666(7)	0.8092(2)	0.3137(3)	21(1)
C(62)	0.7440(7)	0.7966(2)	0.2505(3)	30(1)

C(63)	0.8432(8)	0.8237(2)	0.2147(4)	37(2)
C(64)	0.8680(8)	0.8633(2)	0.2430(4)	38(2)
C(65)	0.7933(8)	0.8755(2)	0.3060(4)	34(2)
C(66)	0.6921(7)	0.8485(2)	0.3411(3)	23(1)

7. Bibliography

[1] K. Dehnicke, J. Strähle, *Angew. Chemie.* **1981**, *93*,451; *Angew. Chem.* Int. Ed. Engl. **1981**, *20*, 413

[2] V. K. Langmuir, *Nucl. Med. Biol.*, **1992**, *19*, 213.

[3] W. A. Nugent, J. M. Mayer, Metal-Ligand Multiple Bonds.

[4] M. Hörner, K.-P. Frank, J. Strähle, *Z. Naturforsch*. **1986**, *41B*, 423.

[5] W. P. Griffith, N. T. McManus, A. C. Skapsi, *J. Chem. Soc., Chem. Comm.*, **1984**, 434.

[6] D. Pawson, W. P. Griffith, *J. Chem. Soc.,Dalton Trans.* , **1975**, 417.

[7] W. P. Griffith, D. Pawson, *J. Chem. Soc., Chem. Comm.*, **1973**, 418.

[8] E. Forsellini. U. Casellato, R. Graziani, L. Magon, *Acta Cryst*. **1982,** *B38,* 3081.

[9] S. Schwarz, M. G. Mestres, E. Niquet, C. F. Barbosa de Silva, J. Strähle, *Z. Naturforsch*. **2004**, *59B*, 167.

[10] L. Pauling, *Die Natur der Chemischen Bindung,* Verlag Chemie, Weinheim, **1968.**

[11] A. Haug, Dissertation, Universität Tübingen **1998**.

[12] S. Schwarz, Dissertation, Universität Tübingen **2004**.

[13] A. F. Clifford, C. S. Kobajashi, *Inorg. Synth.,* **1960,** *6,* 204.

[14] A. Müller, F. Bollmann, E. J. Baran, *Z. Anorg. Allg. Chem.,* **1960,** *370,* 238.

[15] A. L. Spek, PLATON, *FORTRAN-Programm zur Berechnung Krstallographischer Daten,* University of Utrecht **1996.**

[16] E. Keller, SCHAKAL'99, *Programm zur graphischen Darstellung von Kristallstrukturen,* Universität Freiburg **1999**.

[17] W. Herrendorf, HABITUS, *Programm zur Optimierung der Kristallgestalt für die numerische Absorptionskorrektur*, Dissertation, Karlsruhe, **1993**.

[18] W. Haberditzl, Magnetochemie, Akademie-Verlag, Berlin, **1968**.

[19] G. M. Sheldrick, SHELXS97, *FOTRAN-Programm zur Lösung von Kristallstrukturen,* Universität Göttingen, **1997**.

[20] G. M. Sheldrick, SHELXL97, *FOTRAN-Programm zur Verfeinerung von Kristallstrukturen,* Universität Göttingen, **1997**.

[21] A. L. Spek, HELENA, *Program for data reduction of CAD4 data,* Lab. for Crystal- and Structural Chemistry, University of Utrecht, **1993**.

[22] M. Kretschmar, Programm CHECKHKL, Universität Tübingen **1996**.

[23] W. C. Hamilton, *Acta Cryst.,* **1959***, 12,* 609.

Meine akademischen Lehrer waren:

J. Corish, S. Draper, T. Gunnlaugsson, J. Kelly, M. Lyons, D. Mac Dónaill, G. Watson, M. Bridge, D. Grayson, Y. Gun'ko, P. Kruger, A. Morton-Blake, I. Rozas, P. Boyle, T. McMurry, R. Lloyd

K. Albert, G. Häfelinger, H. –J. Meyer, E. Schweda, J. Strähle, N. Kuhn, H. Mayer, H. Oberhammer.

Lebenslauf

Daniel Morrogh

Persönliche Daten:

Geburtsdatum	19. März 1979
Geburtsort	Dublin, Irland
Eltern	William Morrogh Brigitte Morrogh, geb. Seidl
Familienstand	Ledig

Schulbildung:

1983 – 1991	Rathmichael National School, Shankill, Co. Dublin (Grundschule)
1991 – 1997	St. Andrews College Booterstown, Co. Dublin (Gymnasium)
Juni 1997	Leaving Certificate (Abitur)

Universitätsausbildung:

1997 – 2002	University of Dublin, Trinity College Naturwissenschaft (Chemie)
September 2001 – Dezember 2001	Technisches Universität Wien Senior Sophister Forschungs Projekt *Synthesis and characterisation of [μ-Tris(1,8-bis(tetrazol-1-yl)octane)iron(II)]Bis(tetraflouroborate) a novel spin crossover compound*
Juni 2002	BA mod hons (Chem) II.2
Februar 2003 – Dezember 2005	Anfertigung der Doktorarbeit mit dem Titel *Synthese, Charakterisierung und Struktur von mono- und heteronuklearer Nitridokomplexe* bei Prof. Dr. Dr. h. c. J. Strähle am Institut für Anorganische Chemie der Universität Tübingen